AIMS Mathematics, 11(6): 17399–17436.
DOI: 10.3934/math.2026712
Received: 28 March 2026
Revised: 28 March 2026
Accepted: 27 May 2026
Published: 16 June 2026

https://www.aimspress.com/journal/Math

Research article

Stability and bifurcation of a delayed eco-epidemic model with nonlinear prey refuge and additional food

Xin-You Meng*and Peng Fei Zhou

School of Science, Lanzhou University of Technology, Lanzhou, Gansu 730050, China

* **Correspondence:** Email: xymeng@lut.edu.cn.

Abstract: In this paper, we considered an eco-epidemic model incorporating additional food, time delay, and nonlinear prey refuge. First, the analysis began with the model without time delay, focusing on the positivity and boundedness of its solutions. Following this, we established criteria for the local asymptotic stability of all possible equilibria, and obtained some conditions of the global asymptotic stability at the positive equilibrium of model with time-varying delay. Subsequently, we investigated the conditions under which Hopf bifurcation occured in the model with discrete time delay. In addition, we employed the method of multiple time scales to analyze the delay differential system, thereby deriving a time-delay-based control strategy. Specifically, time-varying perturbation was introduced to the delay to suppress oscillation. Finally, the theoretical findings were validated through numerical simulations.

Keywords: Hopf bifurcation; time-varying delay; nonlinear prey refuge; global asymptotical stability; multiple time scales method
Mathematics Subject Classification: 34C60, 92D25, 92D40, 92D55

1. Introduction

The pioneering work of Lotka [1] and Volterra [2] marked the beginning of a sustained focus on the complex dynamics of predator-prey systems, which have since become a cornerstone of theoretical ecology. Scholars have incorporated the traditional predator-prey framework into eco-epidemiological studies, investigating the dynamic relationships that exist between predators and their prey [3, 4]. This cross-disciplinary methodology enhances our comprehension of how disease propagation influences the architecture and operation of food webs [5, 6]. These findings not only advance ecological theory but also offer essential guidance for devising more effective strategies for ecosystem management. Beltrami and Carroll [7] developed an eco-epidemic model where the prey becomes infected by a virus, creating an infected subpopulation. Their work revealed that even a small presence of infectious

agents could destabilize the system. Meng et al. [8] demonstrated that the predator is capable of surviving while transmitting the disease among the prey population. Moreover, Sk and Pal [9] examined a predator-prey system incorporating infected prey. Their findings indicate that elevated fear levels combined with reduced refuge behavior can eradicate the infection from such systems under deterministic and stochastic conditions.

For decades, it is generally accepted that ecosystem diversity has been largely shaped by direct interactions between predators and prey. However, growing empirical evidence reveals that indirect effects can exert equally strong ecological influences such as the prey refuge. Prey refuge refers to a mechanism whereby prey avoids capture by predators through behaviors or environmental conditions. Prey refuge can significantly influence dynamic behaviors of eco-epidemic systems. The functional response was first proposed by Holling [10], suggesting that prey can utilize environmental refuge to avoid capture by predators. In eco-epidemic models, prey refuge is conceptualized as a nonlinear buffering mechanism against predation pressure. By enabling a portion of the prey population to be shielded from predation, the presence of refuge can enhance the resilience of the prey and increase the stability of the overall system. Islam et al. [11] investigated an eco-epidemic predator-prey model that includes nonlinear prey refuge and harvesting of predators. They analyzed local and global stability, and explored Hopf bifurcation as well as transcritical bifurcation in relation to key biological parameters. Their results demonstrate that the infectious disease can be effectively controlled by regulating the basic reproduction number. Jana et al. [12] proposed an eco-epidemic model incorporating time delay and the recovery of infected prey. They found that time delay significantly affects the stability, particularly in suppressing chaotic oscillations and shaping specific stable regions. Erbach et al. [13] revolutionized this paradigm by establishing a generalized predator-prey model with Holling type III function and explicated alternative food dynamics, formally quantifying alternative resource exploitation within the Beverton-Holt framework [14].

Building upon the work of [11] and inspired by references [12, 13], we consider an eco-epidemic system comprising a generalist predator (large wild carnivores, e.g., wolves) and a prey population of captive herbivores (e.g., sheep). The prey is further divided into susceptible and infected populations. We also incorporate a form of nonlinear prey refuge in which the refuge effect intensifies with increasing predator density (modeling the prey's behavior of retreating into enclosures). The following assumptions are given: (i) disease transmission among prey is governed by Holling II functional response; (ii) the predators are generalist predators who can switch to alternative food resources when prey are scarce or extinct; (iii) the gestation delay of predators may fluctuate over time owing to variations in climate, environmental conditions, and individual characteristics. Consequently, incorporating a time-varying gestation delay into the model may provide a more realistic representation. Thus, a time-varying delay eco-epidemic model with additional food, time-varying delay, and nonlinear prey refuge is given as follows:

$$\begin{cases} \dfrac{\mathrm{d}S}{\mathrm{d}t} = rS\left(1-\dfrac{S+I}{K}\right) - \dfrac{\beta S I}{b+S} - m(1-\delta_1 P)SP + \gamma I - q_1 ES, \\ \dfrac{\mathrm{d}I}{\mathrm{d}t} = \dfrac{\beta S I}{b+S} - n(1-\delta_2 P)IP - \gamma I - d_1 I, \\ \dfrac{\mathrm{d}P}{\mathrm{d}t} = \dfrac{\eta P}{1+\eta_0 P} + e_1 m(1-\delta_1 P(t-\tau(t)))S(t-\tau(t))P(t-\tau(t)) \\ \qquad + e_2 n(1-\delta_2 P(t-\tau(t)))I(t-\tau(t))P(t-\tau(t)) - d_2 P - q_2 EP. \end{cases} \tag{1.1}$$

Here S, I, and P represent the densities of susceptible prey, infected prey, and generalist predators at time t, respectively. $\tau(t)$ represents gestation delay and it is a continuously differentiable function. The biological interpretations of the other parameters appearing in model (1.1) are summarized in Table 1. All parameters in model (1.1) are positive. In addition, model (1.1) satisfies the non-negative conditions $S(\xi) = \phi_1(\xi) > 0, I(\xi) = \phi_2(\xi) > 0, P(\xi) = \phi_3(\xi) > 0, \xi \in [-\tau, 0], 0 \leq \tau(t) \leq \tau, \phi_i(\xi) \in \Lambda([-\tau, 0], R^3_+)$, and $i = 1, 2, 3$. Here, R^3_+ denotes the "three-dimensional nonnegative real space," i.e., the set of all three-dimensional vectors whose coordinates are all greater than or equal to zero, which can be written as: $R^3_+ = \left\{(S, I, P) \in R^3 | S \geq 0, I \geq 0, P \geq 0\right\}$.

Compared with the linear function in reference [11], we consider the standard incidence rate $\frac{\beta S I}{b+S}$ in model (1.1). Compared with the linear function in reference [15], we consider the treatment function as a linear function. Compared with the constant harvesting rate of the predator [15, 16], we consider the linear harvesting rate of the susceptible prey and the predator. Compared with the reference [15, 16], one of the most significant improvement of our manuscript lies in the introduction of a generalist predator, which gives a eco-epidemic model with additional food for predators. This modification yields more complex dynamics and better approximates real-world ecosystems. Due to factors such as climate, environmental fluctuations, and individual differences, we also incorporate a time-varying gestation delay for the generalist predator replaced the constant delay, and conduct a detailed analysis of its effects on stability, which is the other of the most significant improvement of our manuscript. In what follows, under the cases of delay-free, constant delay, and time-varying delay, we will systematically discuss the dynamical behavior of time-varying delay eco-epidemic model incorporating additional food, nonlinear prey refuge, and Holling type I functional response, and supplement these theoretical results with numerical simulations.

The remainder of this paper is structured as follows: the positivity and boundedness of solutions for the delay-free model (2.1) are established in Section 2. In Section 3, we derive conditions for the existence and local stability of all six equilibria of model (2.1), and further demonstrate the global stability of the positive equilibrium of model (1.1) by constructing an appropriate Lyapunov function. Section 4 is devoted to analyzing the existence and characteristics of Hopf bifurcation. In Section 5, we apply the method of multiple scales (MMS) to the delay-differential system, based on which a control strategy is developed introducing time-varying perturbations to the delay to suppress oscillations. Numerical simulations confirming the theoretical findings are provided in Section 6. We conclude with a summary and discussion in Section 7.

2. Positivity and boundedness

When $\tau(t) = 0$, the non-delayed model is shown as follows:

$$\begin{cases} \dfrac{\mathrm{d}S}{\mathrm{d}t} = rS(1 - \dfrac{S+I}{K}) - \dfrac{\beta S I}{b+S} - m(1-\delta_1 P)SP + \gamma I - q_1 ES, \\ \dfrac{\mathrm{d}I}{\mathrm{d}t} = \dfrac{\beta S I}{b+S} - n(1-\delta_2 P)IP - \gamma I - d_1 I, \\ \dfrac{\mathrm{d}P}{\mathrm{d}t} = \dfrac{\eta P}{1+\eta_0 P} + e_1 m(1-\delta_1 P)SP + e_2 n(1-\delta_2 P)IP - d_2 P - q_2 EP. \end{cases} \tag{2.1}$$

In this section, we focus on examining key biological properties of the non-delayed model (2.1), specifically, the positivity and boundedness of its solutions.

Theorem 2.1. *For any initial condition* $(S(0), I(0), P(0)) \in \mathbb{R}^3_+ = \{(S, I, P) \in \mathbb{R}^3 \mid S > 0, I > 0, P > 0\}$, *the corresponding solution* $(S(t), I(t), P(t))$ *of model (2.1) remains positive for all* $t > 0$.

Proof. Model (2.1) can be reformulated as

$$\begin{cases} \dfrac{\mathrm{d}S}{\mathrm{d}t} = S\,Y_1(S, I, P), \\ \dfrac{\mathrm{d}I}{\mathrm{d}t} = I Y_2(S, I, P), \\ \dfrac{\mathrm{d}P}{\mathrm{d}t} = P Y_3(S, I, P), \end{cases} \tag{2.2}$$

where,

$$\begin{aligned} Y_1(S, I, P) &= r(1 - \frac{S + I}{K}) - \frac{\beta I}{b + S} - m(1 - \delta_1 P)P + \frac{\gamma I}{S} - q_1 E, \\ Y_2(S, I, P) &= \frac{\beta S}{b + S} - n(1 - \delta_2 P)P - \gamma - d_1, \\ Y_3(S, I, P) &= \frac{\eta}{1 + \eta_0 P} + e_1 m(1 - \delta_1 P)S + e_2 n(1 - \delta_2 P)I - d_2 - q_2 E. \end{aligned}$$

This means

$$\begin{aligned} S(t) &= S(0)e^{\int_0^t Y_1(S(s),I(s),P(s))ds} \geq 0, \\ I(t) &= I(0)e^{\int_0^t Y_2(S(s),I(s),P(s))ds} \geq 0, \\ P(t) &= P(0)e^{\int_0^t Y_3(S(s),I(s),P(s))ds} \geq 0. \end{aligned}$$

The proof of positivity is completed.

Theorem 2.2. *Every solution of model (2.1) is uniformly bounded within the set* Λ.

Proof. By taking the derivative of $Q(t) = S(t) + I(t) + \frac{1}{e_1}P(t)$ with respect to time t, we get

$$\begin{aligned} \frac{\mathrm{d}Q}{\mathrm{d}t} = \frac{\mathrm{d}S}{\mathrm{d}t} + \frac{\mathrm{d}I}{\mathrm{d}t} + \frac{1}{e_1}\frac{\mathrm{d}P}{\mathrm{d}t} =& rS(1 - \frac{S + I}{K}) - q_1 ES - n(1 - \delta_2 P)IP - d_1 I \\ &+ \frac{1}{e_1}(\frac{\eta P}{1 + \eta_0 P} + e_2 n(1 - \delta_2 P)IP - d_2 P - q_2 EP). \end{aligned}$$

Let $L = \min\{d_1, d_2\}$, and η be a normal number. We have

$$\begin{aligned} \frac{\mathrm{d}Q}{\mathrm{d}t} + LQ - \eta Q \leq& S(L + r(1 - \frac{S}{K})) - (d_1 - L)I - \frac{1}{e_1}(d_2 - L)P \\ &+ \frac{1}{e_1}\eta P - \frac{1}{e_1}\eta P - (1 - \frac{e_2}{e_1})nIP(1 - \delta_2 P) \\ \leq& \frac{K}{4r}(r + L)^2 - (d_1 - L)I - \frac{1}{e_1}(d_2 - L)P - (1 - \frac{e_2}{e_1})nIP(1 - \delta_2 P) \\ \leq& \frac{K}{4r}(r + L)^2. \end{aligned}$$

By solving the inequality, we get

$$0 < Q \leq \frac{K}{4rL}(r+L)^2(1-e^{-Lt}) + Q_0 e^{-Lt},$$

here $Q_0 = Q(S(0), I(0), P(0))$. By taking the limit of this inequality as t approaches infinity, we get $0 < Q \leq \frac{K}{4rL}(r+L)^2$. Consequently, every solution of model (2.1) that originates in $\mathbb{R}^3_+$ is confined to the following region:

$$\Lambda = \left\{(S, I, P) : 0 \leq S + I + \frac{1}{e_1}P \leq \frac{K}{4rL}(r+L)^2\right\}.$$

Therefore, every solution of model (2.1) remains uniformly bounded for all $t \geq 0$, and Λ constitutes a positively invariant set.

3. The existence and stability of equilibriums

3.1. Existence of equilibriums

The non-delayed model (2.1) has possible non-negative feasible equilibria as follows:

(i) There always exists a trivial equilibrium, denoted by $E_1(0, 0, 0)$.

(ii) The boundary equilibrium $E_2(S_2, 0, 0)$ and $E_3(0, 0, P_3)$ exists when $q_1E > r$ and $\eta > d_2 + q_2E$, where $S_2 = \frac{(q_1E-r)K}{r}$, $P_3 = \frac{\eta-d_2-q_2E}{(d_2+q_2E)\eta_0}$.

(iii) Assume that $E_4(S_4, I_4, 0)$ is the boundary equilibrium of model (2.1), where S_4 and I_4 fulfill the following relations:

$$\begin{cases} rS_4(1-\dfrac{S_4+I_4}{K}) - \dfrac{\beta S_4 I_4}{b+S_4} + \gamma I_4 - q_1 E S_4 = 0, \\ \dfrac{\beta S_4 I_4}{b+S_4} - \gamma I_4 - d_1 I_4 = 0. \end{cases} \tag{3.1}$$

From the second equation of (3.1), we have

$$S_4 = \frac{b(\gamma + d_1)}{\beta - \gamma - d_1}. \tag{3.2}$$

Inserting (3.2) into the first equation of (3.1) yields

$$I_4 = \frac{\beta(a_1 q_1 bEK(\gamma+d_1) + rb^2(\gamma+d_1)^2 - a_1 rbK(\gamma+d_1))}{a_1(\gamma a_1 K\beta - rb(\gamma+d_1)\beta - a_1\beta K(\gamma+d_1))}, \tag{3.3}$$

where $a_1 = \beta - \gamma - d_1$.

Therefore, if $\frac{b(\gamma+d_1)}{\beta-\gamma-d_1} > 0$ and $\frac{\beta(a_1 q_1 bEK(\gamma+d_1)+rb^2(\gamma+d_1)^2-a_1 rbK(\gamma+d_1))}{a_1(\gamma a_1 K\beta - rb(\gamma+d_1)\beta - a_1\beta K(\gamma+d_1))} > 0$ are satisfied, then model (2.1) has only one predator-free equilibrium $E_4(S_4, I_4, 0)$, which is determined by Eqs (3.2) and (3.3).

(iv) Assume that $E_5(S_5, 0, P_5)$ is the boundary equilibrium of model (2.1), where S_5 and P_5 satisfy the following equations,

$$\begin{cases} rS_5(1-\dfrac{S_5}{K}) - m(1-\delta_1 P_5)S_5 P_5 - q_1 E S_5 = 0, \\ \dfrac{\eta P_5}{1+\eta_0 P_5} + e_1 m(1-\delta_1 P_5)S_5 P_5 - d_2 P_5 - q_2 E P_5 = 0. \end{cases} \tag{3.4}$$

According to the first equation of (3.4), we can obtain

$$S_5 = \frac{(mP_5(1-\delta_1 P_5) + q_1 E - r)K}{r}. \tag{3.5}$$

Substituting (3.5) into the second equation of (3.4), we get

$$c_4 P_5^4 + c_3 P_5^3 + c_2 P_5^2 + c_1 P_5 + c_0 = 0, \tag{3.6}$$

where $c_4 = e_1\eta_0 m^2\delta_1^2 K, c_3 = e_1\delta_1 m^2 K(\delta_1 - \eta_0), c_2 = e_1 mK(-2m\delta_1 + m\eta_0 - m\eta_0\delta_1 + r\delta_1\eta_0 - q_1\eta_0\delta_1 E)$, $c_1 = e_1 mK(m + r\delta_1 + q_1\eta_0 E - q_1\delta_1 E - r\eta_0) - r\eta_0(d_2 + q_2 E), c_0 = e_1 mK(q_1 E - r) + r\eta - r(d_2 + q_2 E)$.

Thus, $c_4 > 0$. Applying Descartes' rule of signs, we find that Eq (3.6) admits exactly one positive root P_5 precisely when one of the following conditions is satisfied.

(1) $c_3 > 0, c_2 > 0, c_1 > 0, c_0 < 0$;

(2) $c_3 > 0, c_2 > 0, c_1 < 0, c_0 < 0$;

(3) $c_3 > 0, c_2 < 0, c_1 < 0, c_0 < 0$;

(4) $c_3 < 0, c_2 < 0, c_1 < 0, c_0 < 0$;

We impose the assumption (H_1): At least one of the conditions (1) – (4) is satisfied. Thus, if (H_1) is satisfied, then model (2.1) has only one disease-free equilibrium $E_5(S_5, 0, P_5)$, which is determined by Eqs (3.5) and (3.6).

(v) The positive equilibrium $E^*(S^*, I^*, P^*)$ exists if and only if S^*, I^*, and P^* satisfy the following equations,

$$\begin{cases} rS^*(1 - \dfrac{S^* + I^*}{K}) - \dfrac{\beta S^* I^*}{b + S^*} - m(1-\delta_1 P^*)S^* P^* + \gamma I^* - q_1 E S^* = 0, \\ \dfrac{\beta S^* I^*}{b + S^*} - n(1-\delta_2 P^*)I^* P^* - \gamma I^* - d_1 I^* = 0, \\ \dfrac{\eta P^*}{1 + \eta_0 P^*} + e_1 m(1-\delta_1 P^*)S^* P^* + e_2 n(1-\delta_2 P^*)I^* P^* - d_2 P^* - q_2 E P^* = 0. \end{cases} \tag{3.7}$$

From the second equation of Eq (3.7), we get

$$S^* = \frac{b(nP^*(1-\delta_2 P^*) + \gamma + d_1)}{\beta - nP^*(1-\delta_2 P^*) - \gamma - d_1}. \tag{3.8}$$

If $\frac{b(nP^*(1-\delta_2 P^*)+\gamma+d_1)}{\beta - nP^*(1-\delta_2 P^*)-\gamma-d_1} > 0$, then $S^* > 0$. Substituting (3.8) into the first and third equation of (3.7), then I^* and P^* are positive solutions of following equation,

$$\begin{cases} \dfrac{rb(K-I^*)(a_1 - nP^*(1-\delta_2 P^*))(nP^*(1-\delta_2 P^*) + a_2) - rb^2(nP^*(1-\delta_2 P^*) + a_2)^2}{K(a_1 - nP^*(1-\delta_2 P^*))^2} + \gamma I^* \\ - \dfrac{(q_1 bE + mbP^*(1-\delta_1 P^*))(nP^*(1-\delta_2 P^*) + a_2)}{a_1 - nP^*(1-\delta_2 P^*)} - I^*(nP^*(1-\delta_2 P^*) + a_2) = 0, \\ \dfrac{\eta}{1 + \eta_0 P^*} + \dfrac{e_1 mb(1-\delta_1 P^*)(nP^*(1-\delta_2 P^*) + a_2)}{a_1 - nP^*(1-\delta_2 P^*)} + e_2 nI^*(1-\delta_2 P^*) - d_2 - q_2 E = 0, \end{cases} \tag{3.9}$$

where $a_2 = d_1 + \gamma$. According to the second equation of (3.9), we can obtain

$$I^* = \frac{d_2 + q_2 E}{e_2 n(1-\delta_2 P^*)} - \frac{\eta}{(1+\eta_0 P^*)e_2 n(1-\delta_2 P^*)} - \frac{e_1 mb(1-\delta_1 P^*)(nP^*(1-\delta_2 P^*) + a_2)}{e_2 n(1-\delta_2 P^*)(a_1 - nP^*(1-\delta_2 P^*))}. \tag{3.10}$$

Substituting (3.10) into the first equation of (3.9), then P^* is the positive root of the following equation,

$$b_8P^{*8} + b_7P^{*7} + b_6P^{*6} + b_5P^{*5} + b_4P^{*4} + b_3P^{*3} + b_2P^{*2} + b_1P^* + b_0 = 0, \tag{3.11}$$

where $b_8, b_7, b_6, b_5, b_4, b_3, b_2, b_1$, and b_0 are all parameters. These forms are too complicated to go into detail here.

It is easy to obtain that $b_8 = mb\eta_0\delta_1\delta_2^3n^3(e_1 + Ke_2) > 0$. By Descartes' rule of signs, Eq (3.11) has a unique positive root P^* precisely when one of the following conditions is satisfied.

(1) $b_7 < 0, b_6 < 0, b_5 < 0, b_4 < 0, b_3 < 0, b_2 < 0, b_1 < 0, b_0 < 0$;

(2) $b_7 > 0, b_6 < 0, b_5 < 0, b_4 < 0, b_3 < 0, b_2 < 0, b_1 < 0, b_0 < 0$;

(3) $b_7 > 0, b_6 > 0, b_5 < 0, b_4 < 0, b_3 < 0, b_2 < 0, b_1 < 0, b_0 < 0$;

(4) $b_7 > 0, b_6 > 0, b_5 > 0, b_4 < 0, b_3 < 0, b_2 < 0, b_1 < 0, b_0 < 0$;

(5) $b_7 > 0, b_6 > 0, b_5 > 0, b_4 > 0, b_3 < 0, b_2 < 0, b_1 < 0, b_0 < 0$;

(6) $b_7 > 0, b_6 > 0, b_5 > 0, b_4 > 0, b_3 > 0, b_2 < 0, b_1 < 0, b_0 < 0$;

(7) $b_7 > 0, b_6 > 0, b_5 > 0, b_4 > 0, b_3 > 0, b_2 > 0, b_1 < 0, b_0 < 0$;

(8) $b_7 > 0, b_6 > 0, b_5 > 0, b_4 > 0, b_3 > 0, b_2 > 0, b_1 > 0, b_0 < 0$.

We introduce the hypothesis (H_2): At least one of conditions (1) – (8) is valid. Under this assumption, Eq (3.11) has a unique positive root P^*. Thus, if $\frac{b(nP^*(1-\delta_2P^*)+\gamma+d_1)}{\beta-nP^*(1-\delta_2P^*)-\gamma-d_1} > 0$, $I^* > 0$, and hypothesis (H_2) are true, then model (2.1) possesses a unique positive equilibrium $E^*(S^*, I^*, P^*)$, where S^*, I^*, and P^* are given by Eqs (3.8), (3.10), and (3.11).

To visualize numerically, we plot 3D visualization of Eq (3.7) with intersecting points for the parametric setup mentioned in Table 1. As illustrated in Figure 1, the three-dimensional representations of Eq (3.7) meet within the positive octant, indicating that model (2.1) possesses a distinct positive equilibrium.

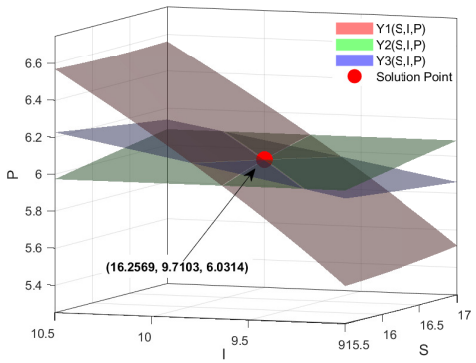

Figure 1. Visualizations of equations with intersection point of Eq (3.7).

Table 1. Descriptions of all the parameters in model (1.1).

Parameters	Descriptions	Values
r	Intrinsic growth rate of susceptible prey	12
K	Carrying capacity of the prey	40
b	Half-saturation constant of the transmission rate	1.2
β	Infection rate among prey	10
γ	Recovery rate of infected prey	1
η	Growth rate of predators from additional food	0.6
η_0	Dependence of predators on additional food	5
δ_1	Refuge coefficient for susceptible prey	0.2
δ_2	Refuge coefficient for infected prey	0.06
m	Predation rate on susceptible prey	0.8
n	Predation rate on infected prey	1.9
e_1	Maximum growth rate of predators from consuming susceptible prey	0.2
e_2	Maximum growth rate of predators from consuming infected prey	0.1
d_1	Death rate of infected prey population	1
d_2	Death rate of predators population	0.5
q_1	Harvest rate of susceptible prey population	0.3
q_2	Harvest rate of predators population	0.2
E	Harvesting effort level	0.8

3.2. The local stability

In this subsection, we analyze the local stability of each equilibrium point. The Jacobian of model (2.1) is given by:

$$J = \begin{bmatrix} j_{11} & j_{12} & j_{13} \\ j_{21} & j_{22} & j_{23} \\ j_{31} & j_{32} & j_{33} \end{bmatrix}, \tag{3.12}$$

where,

$$j_{11} = r - \frac{2r}{K}S - \frac{r}{K}I - \frac{\beta Ib}{(b+S)^2} - m(1-\delta_1 P)P - q_1E, j_{12} = -\frac{r}{K}S - \frac{\beta S}{b+S} + \gamma,$$
$$j_{13} = -mS(1-2\delta_1 P), j_{21} = \frac{\beta Ib}{(b+S)^2}, j_{22} = \frac{\beta S}{b+S} - nP + n\delta_2 P^2 - \gamma - d_1,$$
$$j_{23} = -nI(1-2\delta_2 P), j_{31} = e_1 mP(1-\delta_1 P), j_{32} = e_2 nP(1-\delta_2 P),$$
$$j_{33} = e_1 mS(1-2\delta_1 P) + e_2 nI(1-2\delta_2 P) + \frac{\eta}{(1+\eta_0 P)^2} - d_2 - q_2 E.$$

Theorem 3.1. *If assumption* (H_3)*:* $r - q_1E < 0$, $\eta - d_2 - q_2E < 0$ *is satisfied, then the trivial equilibrium* E_1 *is stable, but instability arises if the opposite inequality holds in any single instance.*

Proof. Employing (3.12), we derive the characteristic equation for the linearization of model (2.1) at E_1:

$$(\lambda - r + q_1E)(\lambda + d_1 + \gamma)(\lambda - \eta + d_2 + q_2E) = 0. \tag{3.13}$$

Thus, the characteristic values around E_1 are $\lambda_1 = r - q_1E, \lambda_2 = -d_1 - \gamma < 0, \lambda_3 = \eta - d_2 - q_2E$. If assumption (H_3) holds, then all roots of the characteristic equation (3.13) have negative real parts,

which indicates that E_1 is locally asymptotically stable. Conversely, if $r - q_1E > 0$ or $\eta - d_2 - q_2E > 0$, then E_1 is unstable.

Theorem 3.2. *If assumption* (H_4)*:* $S_2 > \frac{K}{2} - \frac{KEq_1}{2r}$, $S_2 < \frac{(d_1+r)b}{\beta-d_1-\gamma}$, *and* $S_2 < \frac{d_2+q_2E-\eta}{e_1m}$ *is satisfied, then the boundary equilibrium* E_2 *is stable, while the equilibrium loses stability when the reverse inequality is satisfied for any one of the cases.*

Proof. Making use of (3.12), the characteristic equation of model (2.1) at E_2 reads:

$$(\lambda - r + \frac{2r}{K}S_2 + q_1E)(\lambda - \frac{\beta S_2}{b+S_2} + d_1 + \gamma)(\lambda - e_1mS_2 - \eta + d_2 + q_2E) = 0. \tag{3.14}$$

The characteristic values around E_2 are $\lambda_1 = r - \frac{2r}{K}S_2 - q_1E, \lambda_2 = \frac{\beta S_2}{b+S_2} - d_1 - \gamma$, and $\lambda_3 = e_1mS_2 + \eta - d_2 - q_2E$. If (H_4) holds, then all characteristic values of Eq.(3.14) possess negative real parts, implying that E_2 is locally asymptotically stable. Conversely, if $S_2 < \frac{K}{2} - \frac{KEq_1}{2r}$ or $S_2 > \frac{(d_1+r)b}{\beta-d_1-\gamma}$ or $S_2 > \frac{d_2+q_2E-\eta}{e_1m}$, then E_2 is unstable.

Theorem 3.3. *If assumption* (H_5)*:* $-\delta_1P_3^2 + P_3 > \frac{r-q_1E}{m}, \delta_2P_3^2 - P_3 > \frac{d_1+\gamma}{n}$, *and* $\frac{\eta}{d_2+q_2E} < (1+\eta_0P_3)^2$ *is satisfied, then the boundary equilibrium* E_3 *is stable, but the model becomes unstable whenever the opposite inequality is true for any of the cases.*

Proof. Based on (3.12), the characteristic equation associated with E_3 in model (2.1) takes the form

$$(\lambda - r + mP_3(1-\delta_1P_3) + q_1E)(\lambda - nP_3(\delta_2P_3 - 1) + d_1 + \gamma)(\lambda - \frac{\eta}{(1+\eta_0P_3)^2} + d_2 + q_2E) = 0. \tag{3.15}$$

The characteristic values around E_3 are $\lambda_1 = r - mP_3(1-\delta_1P_3) - q_1E, \lambda_2 = nP_3(\delta_2P_3 - 1) - d_1 - \gamma$, and $\lambda_3 = \frac{\eta}{(1+\eta_0P_3)^2} - d_2 - q_2E$. If (H_5) is true, then all characteristic values of Eq.(3.15) possess negative real parts, implying that E_3 is locally asymptotically stable. Conversely, if $-\delta_1P_3^2 + P_3 < \frac{r-q_1E}{m}$ or $\delta_2P_3^2 - P_3 < \frac{d_1+\gamma}{n}$ or $\frac{\eta}{d_2+q_2E} > (1+\eta_0P_3)^2$, then E_3 is unstable.

Theorem 3.4. *If assumption* (H_6)*:* $r - \frac{2r}{K}S_4 - \frac{r}{K}I_4 - \frac{\beta bI_4}{(b+S_4)^2} - q_1E < 0, e_1mS_4 + e_2nI_4 + \eta - d_2 - q_2E < 0$, *and* $\frac{\beta S_4-(\gamma+d_2)(b+S_4)}{b+S_4} - \frac{((\gamma K-rS_4)(b+S_4)-\beta S_4K)\beta bI_4}{(b+S_4)^3((r-q_1E)K-2rS_4-rI_4)-(b+S_4)\beta bI_4K} < 0$ *is satisfied, then the predator-free equilibrium* $E_4(S_4, I_4, 0)$ *is locally asymptotically stable.*

Proof. From Eq (3.12), the characteristic equation of model (2.1) evaluated at E_4 is given by

$$\begin{aligned}&(\lambda - \frac{\beta S_4 - (\gamma+d_2)(b+S_4)}{b+S_4} + \frac{((\gamma K - rS_4)(b+S_4) - \beta S_4K)\beta bI_4}{(b+S_4)^3((r-q_1E)K - 2rS_4 - rI_4) - (b+S_4)\beta bI_4K})\cdot\\ &(\lambda - r + \frac{2r}{K}S_4 + \frac{r}{K}I_4 + \frac{\beta bI_4}{(b+S_4)^2} + q_1E)\cdot(\lambda - e_1mS_4 - e_2nI_4 - \eta + d_2 + q_2E) = 0.\end{aligned} \tag{3.16}$$

The characteristic values around E_4 are $\lambda_1 = r - \frac{2r}{K}S_4 - \frac{r}{K}I_4 - \frac{\beta bI_4}{(b+S_4)^2} - q_1E, \lambda_2 = e_1mS_4 + e_2nI_4 + \eta - d_2 - q_2E$, and $\lambda_3 = \frac{\beta S_4-(\gamma+d_2)(b+S_4)}{b+S_4} - \frac{((\gamma K-rS_4)(b+S_4)-\beta S_4K)\beta bI_4}{(b+S_4)^3((r-q_1E)K-2rS_4-rI_4)-(b+S_4)\beta bI_4K}$. If (H_6) holds, then all characteristic values of Eq (3.16) possess negative real parts, implying that E_4 is locally asymptotically stable. Conversely, if $r - \frac{2r}{K}S_4 - \frac{r}{K}I_4 - \frac{\beta bI_4}{(b+S_4)^2} - q_1E > 0$ or $e_1mS_4 + e_2nI_4 + \eta - d_2 - q_2E > 0$ or $\frac{\beta S_4-(\gamma+d_2)(b+S_4)}{b+S_4} - \frac{((\gamma K-rS_4)(b+S_4)-\beta S_4K)\beta bI_4}{(b+S_4)^3((r-q_1E)K-2rS_4-rI_4)-(b+S_4)\beta bI_4K}9 > 0$, then E_4 is unstable.

Theorem 3.5. *If assumption* (H_7)*:* $r-\frac{2r}{K}S_5-mP_5(1-\delta_1P_5)-q_1E<0$, $\frac{\beta S_5}{b+S_5}-nP_5(1-\delta_2P_5)-\gamma-d_1<0$, *and* $\frac{e_1m^2KS_5P_5(1-2\delta_1P_5)(1-\delta_1P_5)}{rK-2rS_5-mP_5K(1-\delta_1P_5)-q_1EK}+e_1mS_5(1-2\delta_1P_5)+\frac{\eta}{(1+\eta_0P_5)^2}-d_2-q_2E<0$ *is satisfied, it follows that the disease-free equilibrium* $E_5(S_5,0,P_5)$ *exhibits local asymptotic stability.*

Proof. By virtue of (3.12), the characteristic equation corresponding to E_5 in model (2.1) is:

$$\begin{aligned}&(\lambda-r+\frac{2r}{K}S_5+mP_5(1-\delta_1P_5)+q_1E)(\lambda-\frac{\beta S_5}{b+S_5}+nP_5(1-\delta_2P_5)+\gamma+d_1)(\lambda+d_2+q_2E\\&-\frac{e_1m^2KS_5P_5(1-2\delta_1P_5)(1-\delta_1P_5)}{rK-2rS_5-mP_5K(1-\delta_1P_5)-q_1EK}-e_1mS_5(1-2\delta_1P_5)-\frac{\eta}{(1+\eta_0P_5)^2})=0.\end{aligned}\tag{3.17}$$

The characteristic values around E_5 are $\lambda_1=r-\frac{2r}{K}S_5-mP_5(1-\delta_1P_5)-q_1E$, $\lambda_2=\frac{\beta S_5}{b+S_5}-nP_5(1-\delta_2P_5)-\gamma-d_1$, and $\lambda_3=\frac{e_1m^2KS_5P_5(1-2\delta_1P_5)(1-\delta_1P_5)}{rK-2rS_5-mP_5K(1-\delta_1P_5)-q_1EK}+e_1mS_5(1-2\delta_1P_5)+\frac{\eta}{(1+\eta_0P_5)^2}-d_2-q_2E$. If assumption (H_7) holds, then all characteristic values of Eq (3.17) possess negative real parts, implying that E_5 is locally asymptotically stable. Conversely, if $r-\frac{2r}{K}S_5-mP_5(1-\delta_1P_5)-q_1E>0$ or $\frac{\beta S_5}{b+S_5}-nP_5(1-\delta_2P_5)-\gamma-d_1>0$ or $\frac{e_1m^2KS_5P_5(1-2\delta_1P_5)(1-\delta_1P_5)}{rK-2rS_5-mP_5K(1-\delta_1P_5)-q_1EK}+e_1mS_5(1-2\delta_1P_5)+\frac{\eta}{(1+\eta_0P_5)^2}-d_2-q_2E>0$, then E_5 is unstable.

Theorem 3.6. *Under assumption* (H_8)*, as specified in the proof, then the positive equilibrium* $E^*(S^*,I^*,P^*)$ *is locally asymptotically stable.*

Proof. The Jacobian matrix at equilibrium E^* is given by

$$J(E^*)=\begin{bmatrix}e_{11}&e_{12}&e_{13}\\e_{21}&e_{22}&e_{23}\\e_{31}&e_{32}&e_{33}\end{bmatrix},\tag{3.18}$$

where,

$$\begin{aligned}&e_{11}=-\frac{rS^*}{K}+\frac{\beta S^*I^*}{(b+S^*)^2}-\frac{\gamma I^*}{S^*},e_{12}=-\frac{rS^*}{K}-\frac{\beta S^*}{b+S^*}+\gamma,e_{13}=mS^*(2\delta_1P^*-1),\\&e_{21}=\frac{\beta bI^*}{(b+S^*)^2},e_{22}=0,e_{23}=nI^*(2\delta_2P^*-1),e_{31}=e_1mP^*(1-\delta_1P^*),\\&e_{32}=e_2nP^*(1-\delta_2P^*),e_{33}=-P^*(\frac{\eta\eta_0}{(1+\eta_0P^*)^2}+e_1m\delta_1S^*+e_2n\delta_2I^*).\end{aligned}$$

The characteristic equation of $J(E^*)$ is given by

$$\lambda^3+M_1\lambda^2+M_2\lambda+M_3=0,\tag{3.19}$$

where $M_1=-(e_{11}+e_{33})$, $M_2=e_{11}e_{33}-e_{12}e_{21}-e_{13}e_{31}-e_{23}e_{32}$, and $M_3=e_{11}e_{23}e_{32}+e_{12}e_{21}e_{33}-e_{12}e_{23}e_{31}-e_{13}e_{21}e_{32}$.

From the Routh-Hurwitz criteria, if assumption $(H_8):M_1>0,M_2>0,M_1M_2-M_3>0$ holds, then Eq (3.19) has three negative roots, the positive equilibrium E^* of model (2.1) is locally asymptotically stable.

3.3. The global asymptotical stability

To analyze the global stability of the positive equilibrium $E^*(S^*, I^*, P^*)$, we employ Lemma 1 [17], which establishes key properties of nonnegative, uniformly continuous, and integrable functions. A necessary and sufficient condition for system stability is the positive definiteness of matrix H.

Lemma 1. *If f is defined on $[0, +\infty)$ and nonnegative such that f is uniformly continuous and integrable $[0, +\infty)$, then $\lim_{t\to+\infty} f(t) = 0$.*

Theorem 3.7. *If every principal minor of the 6×6 matrix $H = (h_{mn})$ is positive, then the positive equilibrium $E^*(S^*, I^*, P^*)$ of system (1.1) is globally asymptotically stable provided that $\tau'(t) \leq \bar{M}$, where $\bar{M}$ is a positive constant, and the definition of H is provided in the following analysis.*

Proof. We start by introducing the following Lyapunov function:

$$\begin{aligned} V(S, I, P) =& S - S^* - S^* \ln \frac{S}{S^*} + I - I^* - I^* \ln \frac{I}{I^*} + P - P^* - P^* \ln \frac{P}{P^*} \\ &+ \int_{t-\tau(t)}^{t} ((S(s) - S^*)^2 + (I(s) - I^*)^2 + (P(s) - P^*)^2) ds. \end{aligned} \tag{3.20}$$

In order to read easily, we denote $S(t - \tau(t)), I(t - \tau(t))$, and $P(t - \tau(t))$ as $S_{\tau_t}, I_{\tau_t}, P_{\tau_t}$. Eq.(3.20) takes the derivative of t,

$$\begin{aligned} \frac{\mathrm{d}V}{\mathrm{d}t} =& (\frac{\beta I^*}{(b + S)(b + S^*)} - \frac{r}{K} + 1)(S - S^*)^2 + (I - I^*)^2 \\ &+ (1 - \frac{\eta\eta_0}{(1 + \eta_0 P)(1 + \eta_0 P^*)})(P - P^*)^2 - (1 - \tau'(t))(S_{\tau_t} - S^*)^2 \\ &- (1 - \tau'(t))(I_{\tau_t} - I^*)^2 - (1 - \tau'(t))(P_{\tau_t} - P^*)^2 \\ &+ (\frac{\gamma}{S} - \frac{r}{K} - \frac{\beta(S^* + 2b)}{(b + S)(b + S^*)})(S - S^*)(I - I^*) \\ &+ (\delta_1 m(P + P^*) - m)(S - S^*)(P - P^*) + (\delta_2 n(P + P^*) - n)(I - I^*)(P - P^*) \\ &+ \frac{e_1 m(P^* - \delta_1 P_{\tau_t}^2)}{P}(P - P^*)(S_{\tau_t} - S^*) + \frac{e_2 n(P^* - \delta_2 P_{\tau_t}^2)}{P}(P - P^*)(I_{\tau_t} - I^*) \\ &+ \frac{e_1 m(S_{\tau_t} - \delta_1 S^*(P_{\tau_t} + P^*) + e_2 n(I_{\tau_t} - \delta_2 I^*(P_{\tau_t} + P^*))}{P}(P - P^*)(P_{\tau_t} - P^*). \end{aligned} \tag{3.21}$$

Based on the important inequality and the uniform boundedness of the solutions, we obtain:

$$\begin{aligned} \frac{\mathrm{d}V}{\mathrm{d}t} \leq& \big[\frac{2\gamma}{S} + 2\delta_1 m(P + P^*) + \frac{\beta I^*}{(b + S)(b + S^*)} + 1 - \frac{r}{K}\big](S - S^*)^2 \\ &+ \big[\frac{2\gamma}{S} + 2\delta_2 n(P + P^*) + 1 - \frac{2r}{K}\big](I - I^*)^2 \\ &+ \big[1 + 2(\delta_1 m + \delta_2 n)(P + P^*) + \frac{2P^*(e_1 m + e_2 n) + 2(e_1 m S_{\tau_t} + e_2 n I_{\tau_t})}{P} \\ &- \frac{\eta\eta_0}{(1 + \eta_0 P)(1 + \eta_0 P^*)}\big](P - P^*)^2 \\ &- (1 - \bar{M})(S_{\tau_t} - S^*)^2 - (1 - \bar{M})(I_{\tau_t} - I^*)^2 - (1 - \bar{M})(P_{\tau_t} - P^*)^2 \end{aligned}$$

$$
\begin{aligned}
&\leq \Big[\frac{2\gamma}{\underline{S}} + 2\delta_1 m\Big(\frac{Ke_1}{4rL}(r+L)^2 + P^*\Big) + \frac{\beta I^*}{b(b+S^*)} + 1 - \frac{r}{K}\Big](S-S^*)^2 \\
&\quad + \Big[\frac{2\gamma}{\underline{S}} + 2\delta_2 n\Big(\frac{Ke_1}{4rL}(r+L)^2 + P^*\Big) + 1 - \frac{2r}{K}\Big](I-I^*)^2 \\
&\quad + \Big[1 + 2(\delta_1 m + \delta_2 n)\Big(\frac{Ke_1}{4rL}(r+L)^2 + P^*\Big) - \frac{\eta\eta_0}{(1+\frac{K\eta_0 e_1}{4rL}(r+L)^2)(1+\eta_0 P^*)} \\
&\quad + \frac{2P^*(e_1 m + e_2 n) + 2(e_1 m + e_2 n)\frac{K}{4rL}(r+L)^2}{\underline{P}}\Big](P-P^*)^2 \\
&\quad - (1-\bar{M})(S_{\tau_t} - S^*)^2 - (1-\bar{M})(I_{\tau_t} - I^*)^2 - (1-\bar{M})(P_{\tau_t} - P^*)^2 \\
&\leq - h_{11}(S-S^*)^2 - h_{22}(I-I^*)^2 - h_{33}(P-P^*)^2 - h_{44}(S_{\tau_t} - S^*)^2 \\
&\quad - h_{55}(I_{\tau_t} - I^*)^2 - h_{66}(P_{\tau_t} - P^*)^2 \\
&\leq - R^{\mathrm{T}} H R,
\end{aligned}
\tag{3.22}
$$

where $R^{\mathrm{T}} = (|S-S^*|, |I-I^*|, |P-P^*|, |S_{\tau_t} - S^*|, |I_{\tau_t} - I^*|, |P_{\tau_t} - P^*|)$, $H = (h_{mn}), m, n = 1, 2, 3, 4, 5, 6$, $\underline{S}$ and $\underline{P}$ are the lower bounds of S(t) and P(t), respectively.

$$
\begin{aligned}
h_{11} =& \frac{r}{K} - \frac{2\gamma}{\underline{S}} - 2\delta_1 m\Big(\frac{Ke_1}{4rL}(r+L)^2 + P^*\Big) - \frac{\beta I^*}{b(b+S^*)} - 1, \\
h_{22} =& \frac{2r}{K} - \frac{2\gamma}{\underline{S}} - 2\delta_2 n\Big(\frac{Ke_1}{4rL}(r+L)^2 + P^*\Big) - 1, h_{44} = h_{55} = h_{66} = 1 - \bar{M}, \\
h_{33} =& \frac{\eta\eta_0}{(1+\frac{K\eta_0 e_1}{4rL}(r+L)^2)(1+\eta_0 P^*)} - 1 - 2(\delta_1 m + \delta_2 n)\Big(\frac{Ke_1}{4rL}(r+L)^2 + P^*\Big) \\
& - \frac{2P^*(e_1 m + e_2 n) + 2(e_1 m + e_2 n)\frac{K}{4rL}(r+L)^2}{\underline{P}}, h_{ij} = 0, i \neq j, i, j = 1, 2, 3, 4, 5, 6.
\end{aligned}
$$

The positive definiteness of matrix H is equivalent to all of its leading principal minors being positive. The principal minors of matrix H are $D_1 = h_{11}, D_2 = h_{11}h_{22}, D_3 = h_{11}h_{22}h_{33}, D_4 = h_{11}h_{22}h_{33}h_{44}, D_5 = h_{11}h_{22}h_{33}h_{44}h_{55}$, and $D_6 = h_{11}h_{22}h_{33}h_{44}h_{55}h_{66}$.

We can obtain

$$
\frac{\mathrm{d}V}{\mathrm{d}t} \leq -R^{\mathrm{T}} H R \leq -\nu(|S(s) - S^*|^2 + |I(s) - I^*|^2 + |P(s) - P^*|^2), \tag{3.23}
$$

with ν being the smallest eigenvalue. Equation (3.23) then yields

$$
V(S, I, P) + \nu(|S(s) - S^*|^2 + |I(s) - I^*|^2 + |P(s) - P^*|^2) \leq V(S(0), I(0), P(0)). \tag{3.24}
$$

By definition of $V(S, I, P)$ and Eq (3.24), $S(t), I(t)$, and $P(t)$ are bounded uniformly on $[0, +\infty)$ and the same is also for $\frac{\mathrm{d}S}{\mathrm{d}t}$, $\frac{\mathrm{d}I}{\mathrm{d}t}$, and $\frac{\mathrm{d}P}{\mathrm{d}t}$ on $[0, +\infty)$. From Lemma 1 and Eq (3.24), it can be inferred that

$$
\lim_{t\to+\infty} |S(t) - S^*|^2 = 0, \lim_{t\to+\infty} |I(t) - I^*|^2 = 0, \lim_{t\to+\infty} |P(t) - P^*|^2 = 0.
$$

Thus, the global asymptotic stability of E^* is established. This completes the proof.

4. Hopf bifurcation

4.1. Existence of Hopf bifurcation

Our initial focus is on the existence of Hopf bifurcation in model (1.1) under the condition that $\tau(t)$ takes the constant value $\bar{\tau}$, with $0 < \bar{\tau} < \tau$. Thus, model (1.1) is rewritten as follows:

$$\begin{cases} \dfrac{\mathrm{d}S}{\mathrm{d}t} = rS(1 - \dfrac{S+I}{K}) - \dfrac{\beta S I}{b+S} - m(1-\delta_1 P)SP + \gamma I - q_1 ES, \\ \dfrac{\mathrm{d}I}{\mathrm{d}t} = \dfrac{\beta S I}{b+S} - n(1-\delta_2 P)IP - \gamma I - d_1 I, \\ \dfrac{\mathrm{d}P}{\mathrm{d}t} = \dfrac{\eta P}{1+\eta_0 P} + e_1 m(1-\delta_1 P(t-\bar{\tau}))S(t-\bar{\tau})P(t-\bar{\tau}) \\ \quad + e_2 n(1-\delta_2 P(t-\bar{\tau}))I(t-\bar{\tau})P(t-\bar{\tau}) - d_2 P - q_2 EP. \end{cases} \tag{4.1}$$

The linearized model (4.1) at $E^*(S^*, I^*, P^*)$ can be transformed into

$$\begin{pmatrix} \frac{\mathrm{d}S}{\mathrm{d}t} \\ \frac{\mathrm{d}I}{\mathrm{d}t} \\ \frac{\mathrm{d}P}{\mathrm{d}t} \end{pmatrix} = \begin{pmatrix} a_{11} & a_{12} & a_{13} \\ a_{21} & 0 & a_{23} \\ 0 & 0 & a_{33} \end{pmatrix} \begin{pmatrix} S(t) \\ I(t) \\ P(t) \end{pmatrix} + \begin{pmatrix} 0 & 0 & 0 \\ 0 & 0 & 0 \\ b_{31} & b_{32} & b_{33} \end{pmatrix} \begin{pmatrix} S(t-\bar{\tau}) \\ I(t-\bar{\tau}) \\ P(t-\bar{\tau}) \end{pmatrix}, \tag{4.2}$$

where $a_{11} = e_{11}, a_{12} = e_{12}, a_{13} = e_{13}, a_{21} = e_{21}, a_{23} = e_{23}, b_{31} = e_{31}, b_{32} = e_{32}$, $a_{33} = \frac{\eta}{(1+\eta_0 P^*)^2} - d_2 - q_2 E$, and $b_{33} = e_1 m S^*(1 - 2\delta_1 P^*) + e_2 n I^*(1 - 2\delta_2 P^*)$.

The characteristic equation for model (4.2) evaluated at the positive equilibrium $E^*(S^*, I^*, P^*)$ is given by

$$\lambda^3 + P_2\lambda^2 + P_1\lambda + P_0 + e^{-\lambda\bar{\tau}}(Q_2\lambda^2 + Q_1\lambda + Q_0) = 0, \tag{4.3}$$

where $P_2 = -(a_{11} + a_{33}), P_1 = a_{11}a_{33} - a_{12}a_{21}, P_0 = a_{12}a_{21}a_{33}, Q_2 = -b_{33}, Q_1 = a_{11}b_{33} - a_{23}b_{32} - a_{13}b_{31}$, and $Q_0 = a_{11}a_{23}b_{32} + a_{12}a_{21}b_{33} - a_{12}a_{23}b_{31} - a_{13}a_{21}b_{32}$.

Suppose that $\lambda = i\omega$ (with $\omega > 0$) is a solution to Eq (4.3). Substituting this into the equation and extracting the real and imaginary components yields

$$\begin{cases} P_1\omega - \omega^3 = Q_0 \sin(\omega\bar{\tau}) - Q_2\omega^2 \sin(\omega\bar{\tau}) - Q_1\omega\cos(\omega\bar{\tau}), \\ P_0 - P_2\omega^2 = Q_2\omega^2\cos(\omega\bar{\tau}) - Q_0\cos(\omega\bar{\tau}) - Q_1\omega\sin(\omega\bar{\tau}). \end{cases} \tag{4.4}$$

Squaring each of the two equations in (4.4) and then adding them together yields

$$\omega^6 + r_2\omega^4 + r_1\omega^2 + r_0 = 0, \tag{4.5}$$

where $r_2 = P_2^2 - 2P_1 - Q_2^2, r_1 = P_1^2 - Q_1^2 - 2P_0P_2 + 2Q_0Q_2$, and $r_0 = P_0^2 - Q_0^2$.

Let $\omega^2 = v$, we can rewrite Eq (4.5) as

$$f(v) = v^3 + r_2v^2 + r_1v + r_0 = 0. \tag{4.6}$$

By differentiating both sides of the equation with respect to v, we obtain: $f'(v) = 3v^2 + 2r_2v + r_1 = 0$, and the roots of $f'(v) = 0$ can be expressed as $v_{1,2} = \frac{-r_2 \pm \sqrt{r_2^2 - 3r_1}}{3}$.

Following the approach in [18] and employing Fan's formula [19], we obtain the discriminant of Eq (4.6) as: $\Delta = \tilde{B}^2 - 4\tilde{A}\tilde{C}$, here $\tilde{A} = r_2^2 - 3r_1, \tilde{B} = r_1r_2 - 9r_0, \tilde{C} = r_1^2 - 3r_0r_2$.

Lemma 2. *From Eq (4.6), we have the following conclusions:*

(i) If condition (H_9)*:* $r_0 \geq 0$ *and* $r_2^2 - 3r_1 \leq 0$ *is satisfied, then* $f(v)$ *is strictly increasing for all* $v \in [0, +\infty)$*. Consequently,* $f(v) = 0$ *admits no positive solutions in this interval, implying that Eq (4.6) has no positive root.*

(ii) If $\Delta > 0$*, then Eq (4.6) only has one positive root.*

(iii) If $\Delta = 0$*, then Eq (4.6) has two positive roots.*

(iv) If $\Delta < 0$*, then Eq (4.6) has three positive roots.*

Without loss of generality, suppose that Eq (4.6) has three positive roots, namely v_1, v_2, and v_3, then Eq (4.5) possesses the following three roots: $\omega_1 = \sqrt{v_1}, \omega_2 = \sqrt{v_2}$, and $\omega_3 = \sqrt{v_3}$. Based on Eq (4.4), we have

$$\bar{\tau}_k^j = \frac{1}{\omega_k} \arccos[\frac{(P_0 - P_2\omega_k^2)(Q_2\omega_k^2 - Q_0) + Q_1\omega_k^2(\omega_k^2 - P_1)}{(Q_2\omega_k^2 - Q_0)^2 + Q_1^2\omega_k^2}] + \frac{2\pi j}{\omega_k}, k = 1, 2, 3, j = 0, 1, 2, \cdots .$$

Define $\bar{\tau}_1^0 = min\{\bar{\tau}_k^j, k = 1, 2, 3, j = 0, 1, 2, \cdots\}$. Thus, when $\bar{\tau} = \bar{\tau}_1^0$, then $\pm i\omega_1$ is a pair of pure imaginary roots of Eq (4.3), and the other roots have non-negative real parts.

Let $\lambda(\bar{\tau}) = \alpha(\bar{\tau}) + i\beta(\bar{\tau})$ be the root of Eq (4.3) when $\bar{\tau} = \bar{\tau}_1^0$, satisfying $\alpha(\bar{\tau}_1^0) = 0$ and $\beta(\bar{\tau}_1^0) = \omega_1$.

Theorem 4.1. *If* $v_1 = \omega_1^2$ *and* $f'(v_1) \neq 0$ *hold, then* $\frac{dRe(\lambda(\bar{\tau}))}{d\bar{\tau}}|_{\lambda=i\omega_0} \neq 0$.

Proof. Taking the derivative of Eq (4.3) with respect to $\bar{\tau}$ yields

$$\left[\frac{d\lambda}{d\bar{\tau}}\right]^{-1} = \frac{(3\lambda^2 + 2P_2\lambda + P_1)e^{\lambda\bar{\tau}} + 2Q_2\lambda + Q_1}{\lambda(Q_2\lambda^2 + Q_1\lambda + Q_0)} - \frac{\bar{\tau}}{\lambda}, \tag{4.7}$$

Substituting $\lambda = i\omega_0$ into Eq (4.7) and extracting the real part yields

$$\begin{aligned} Re\left[\frac{d\lambda}{d\bar{\tau}}\right]_\lambda^{-1} &= \frac{3\omega_0^4 + 2(P_2^2 - 2P_1 - Q_2^2)\omega_0^2 + P_1^2 - 2P_0P_2 + 2Q_0Q_2 - Q_1^2}{\omega_0^2((Q_0 - Q_2\omega_0^2)^2 + Q_1^2\omega_0^2)} \\ &= \frac{f'(v_k)}{\omega_0^2((Q_0 - Q_2\omega_0^2)^2 + Q_1^2\omega_0^2)}. \end{aligned}$$

So we have

$$sign\left[\frac{d}{d\bar{\tau}}(Re(\lambda))\right]_{\lambda=i\omega_0} = sign\left[Re(\frac{d\lambda}{d\bar{\tau}})^{-1}\right]_{\lambda=i\omega_0} = sign\{f'(v_1)\} \neq 0.$$

On the basis of the foregoing analysis, we now state the following theorem concerning the stability of E^* and the occurrence of Hopf bifurcation.

Theorem 4.2. *For the delayed model (4.1) with* $\bar{\tau} > 0$*, the following conclusions can be drawn:*

(i) Under assumption (H_9)*, the positive equilibrium* E^* *remains locally asymptotically stable for any* $\bar{\tau} > 0$.

(ii) When $\Delta < 0$ *is satisfied,* E^* *is locally asymptotically stable for* $\tau \in [0, \bar{\tau})$*, but becomes unstable once* τ *exceeds* $\bar{\tau}$.

(iii) Provided that $\Delta < 0$ *and* $f'(v_1) \neq 0$ *hold, model (4.1) experiences a Hopf bifurcation at* E^* *precisely when* $\tau = \bar{\tau}$.

4.2. The properties of Hopf bifurcation

When $\tau = \bar{\tau}$, the existence of Hopf bifurcation has been discussed in Theorem 4.2. Next, we will employ the ideas from reference [20] to explore the properties of Hopf bifurcation.

Let $\tau = \bar{\tau} + \mu$, $\mu \in R$. Then, $\mu = 0$ is a Hopf bifurcation value for model (4.1). Defining the phase space $\psi = C([-1, 0], R^3)$ and implementing the time transformation $\tilde{t} = \frac{t}{\tau}$ normalizes all time-dependent terms. Define $U_1(t) = S(t) - S^*, U_2(t) = I(t) - I^*, U_3(t) = P(t) - P^*, U(t) = (U_1(t), U_2(t), U_3(t))^{\mathrm{T}} \in R^3$ and $t = \tilde{t}$. Model (4.2) admits a representation as a functional differential equation in ψ,

$$\dot{U}(t) = L_\mu(U_t) + F(\mu, U_t), \tag{4.8}$$

where $L_\mu : \psi \to R^3$ and $F : R \times \psi \to R^3$.

Let $\varphi(\theta) = (\varphi_1(\theta), \varphi_2(\theta), \varphi_3(\theta))^{\mathrm{T}} \in R^3$, where $\theta \in [-1, 0]$, such that

$$L_\mu(\varphi) = (\bar{\tau} + \mu)L_1\varphi(0) + (\bar{\tau} + \mu)L_2\varphi(-1), \tag{4.9}$$

and

$$F(\mu, \varphi) = (\bar{\tau} + \mu) \begin{pmatrix} F_1(\varphi) \\ F_2(\varphi) \\ F_3(\varphi) \end{pmatrix}, \tag{4.10}$$

where L_1 and L_2 are defined by Eq (4.2), for the meanings of the remaining parameters in the Eq (4.10), see Eq (7.1) in the Appendix.

According to the Riesz representation theorem [21], there exists a matrix function $\eta(\theta, \mu) \in C([-1, 0], R^3)$, such that

$$L_\mu(\varphi) = \int_{-1}^{0} d\eta(\theta, \mu)\varphi(\theta), \varphi \in \psi, \tag{4.11}$$

where $\eta(\theta, 0) = \bar{\tau}L_1\delta(\theta) - \bar{\tau}L_2\delta(\theta + 1)$, $\delta(\theta)$ is a Dirac delta function, that is

$$\delta(\theta) = \begin{cases} 0, \theta \neq 0, \\ 1, \theta = 0. \end{cases}$$

For $\varphi \in C([-1, 0], R^3)$, we define:

$$A(\mu)\varphi = \begin{cases} \frac{\mathrm{d}\varphi(\theta)}{\mathrm{d}\theta}, & \theta \in [-1, 0), \\ \int_{-1}^{0} d\eta(\mu, s)\varphi(s), & \theta = 0, \end{cases}$$

$$R(\mu)\varphi = \begin{cases} 0, & \theta \in [-1, 0), \\ F(\mu, \varphi), & \theta = 0. \end{cases}$$

Therefore, Eq (4.8) can be transformed into

$$\dot{U}(t) = A_\mu(U_t) + R_\mu U_t. \tag{4.12}$$

For $\Psi \in \psi^* = C^*([-1, 0], R^3)$, we define:

$$A^*(\mu)\Psi(s) = \begin{cases} -\frac{\mathrm{d}\Psi(s)}{\mathrm{d}s}, & s \in (0, 1], \\ \int_{-1}^{0} \Psi(-\xi)d\eta(\xi, 0), & s = 0, \end{cases}$$

and establish a bilinear inner product:

$$\langle \Psi(s), \varphi(\theta)\rangle = \bar{\Psi}(0)\varphi(0) - \int_{-1}^{0}\int_{0}^{\theta} \bar{\Psi}(\xi-\theta)d\eta(\theta)\varphi(\xi)d\xi, \Psi(s)\in C^*, \varphi(\theta)\in C,$$

where $\eta(\theta) = \eta(\theta, 0)$. $A(0)$ and $A^*(0)$ are adjoint operators. According to Theorem 4.2, $\pm i\omega_k\bar{\tau}$ are eigenvalues of $A(0)$; consequently, they are also eigenvalues of $A^*(0)$. Let $q(\theta) = (1, q_1, q_2)^{\mathrm{T}} e^{i\omega_k\bar{\tau}\theta}$ be the eigenvector of $A(0)$ corresponding to the eigenvalue $i\omega_k\bar{\tau}$, then $A(0)q(\theta) = i\omega_k\bar{\tau}q(\theta)$. Furthermore, we have

$$(\bar{\tau}+\mu)\begin{pmatrix} a_{11}-i\omega_k & a_{12} & a_{13} \\ a_{21} & -i\omega_k & a_{23} \\ b_{31}e^{-i\omega_k\bar{\tau}} & b_{32}e^{-i\omega_k\bar{\tau}} & a_{33}-i\omega_k+b_{33}e^{-i\omega_k\bar{\tau}}\end{pmatrix}\begin{pmatrix}1\\ q_1\\ q_2\end{pmatrix} = 0,$$

Solving the above equation, we have $(1, q_1, q_2)^{\mathrm{T}} = (1, \frac{a_{23}a_{11}-a_{21}a_{13}-i\omega_k a_{23}}{-i\omega_k a_{13}-a_{23}a_{12}}, \frac{\omega_k^2+i\omega_k a_{11}+a_{21}a_{12}}{-i\omega_k a_{13}-a_{23}a_{12}})^{\mathrm{T}}$.

Similarly, assuming that $q^*(s) = D(1, q_1^*, q_2^*)e^{-i\omega_k\bar{\tau}s}$ is the eigenvector of $A^*(0)$ corresponding to the eigenvalue $-i\omega_k\bar{\tau}$, then $A^*(0)q^*(s) = -i\omega_k\bar{\tau}q^*(s)$. From the above definitions, we have $(1, q_1^*, q_2^*)^{\mathrm{T}} = (1, \frac{-a_{12}}{i\omega_k\bar{\tau}} - \frac{b_{32}}{i\omega_k\bar{\tau}}\cdot\frac{(\omega_k\bar{\tau})^2+a_{21}a_{12}-i\omega_k\bar{\tau}a_{11}}{i\omega_k\bar{\tau}b_{31}-a_{21}b_{32}}, \frac{(\omega_k\bar{\tau})^2+a_{21}a_{12}-i\omega_k\bar{\tau}a_{11}}{e^{-i\omega_k\bar{\tau}}(i\omega_k\bar{\tau}b_{31}-a_{21}b_{32})})^{\mathrm{T}}$. Moreover, $\langle q^*, q\rangle$ can be expressed as

$$\begin{aligned}\langle q^*, q\rangle =& \bar{q}^*(0)q(0) - \int_{-1}^{0}\int_{0}^{\theta}\bar{q}^*(\xi-\theta)d\eta(\theta)q(\xi)d\xi\\ =&\bar{D}[(1, q_1^*, q_2^*)(1, q_1, q_2)^{\mathrm{T}} - \int_{-1}^{0}\int_{0}^{\theta}(1, \bar{q}_1^*, \bar{q}_2^*)e^{-i\omega_k(\xi-\theta)\bar{\tau}}d\eta(\theta)(1, q_1, q_2)^{\mathrm{T}}e^{i\omega_k\xi\bar{\tau}}d\xi]\\ =&\bar{D}[1+q_1\bar{q}_1^*+q_2\bar{q}_2^*+\bar{\tau}(b_{31}+b_{32}q_1+b_{33}q_2)\bar{q}_2^*e^{-i\omega_k\bar{\tau}}].\end{aligned}$$

Thus, we choose $\bar{D} = [1+q_1\bar{q}_1^*+q_2\bar{q}_2^*+\bar{\tau}(b_{31}+b_{32}q_1+b_{33}q_2)\bar{q}_2^*e^{-i\omega_k\bar{\tau}}]^{-1}$, satisfying $\langle q^*, q\rangle = 1$.

Next, we adopt the methodology [20] to compute the coordinates of the center manifold C_0 at $\mu = 0$. When $\mu = 0$, let U_t be a solution to Eq (4.8). Define:

$$p(t) = \langle q^*, U_t\rangle, W(t,\theta) = U_t(\theta) - 2Re\{p(t)q(\theta)\}. \tag{4.13}$$

Restricted to the center manifold C_0, we obtain

$$W(t,\theta) = W(p(t), \bar{p}(t), \theta) = W_{20}(\theta)\frac{p^2}{2} + W_{11}(\theta)p\bar{p} + W_{02}(\theta)\frac{\bar{p}^2}{2} + \cdots, \tag{4.14}$$

where p and $\bar{p}$ represent the local coordinates on the center manifold along the directions of q^* and $\bar{q}^*$, respectively. When U_t is real-valued, W must be real-valued. For real solutions of Eq (4.12), when $\mu = 0$, we have

$$\begin{aligned}\dot{p}(t) =& \left\langle q^*, \dot{U}(t)\right\rangle = \langle q^*, A(0)U_t + R(0)U_t\rangle = \langle A^*(0)q^*, U_t\rangle + \bar{q}^*(0)F(0, U_t)\\ =&i\omega_k\bar{\tau}p(t) + \bar{q}^*(0)F(0, W(p,\bar{p},0) + 2Re\{p(t)q(0)\})\\ \overset{def}{=}& i\omega_k\bar{\tau}p(t) + \bar{q}^*(0)F_0(p,\bar{p}).\end{aligned} \tag{4.15}$$

Equation (4.15) can be rewritten as

$$\dot{p}(t) = i\omega_k\bar{\tau}p(t) + g(p,\bar{p}),$$

where,

$$g(p,\bar{p}) = \bar{q}^*(0)F_0(p,\bar{p}) = g_{20}(\theta)\frac{p^2}{2} + g_{11}(\theta)p\bar{p} + g_{02}(\theta)\frac{\bar{p}^2}{2} + g_{21}(\theta)\frac{p^2\bar{p}}{2} + \cdots. \tag{4.16}$$

According to Eq (4.13), we can obtain

$$\begin{aligned}\dot{W} = \dot{U}_t - \dot{p}q - \dot{\bar{p}}\bar{q} &= \begin{cases} AW - 2Re\left\{\bar{q}^*(0)F_0q(\theta)\right\}, & \theta \in [-1,0), \\ AW - 2Re\left\{\bar{q}^*(0)F_0q(0)\right\} + F_0, & \theta = 0, \end{cases} \\ &\overset{def}{=} AW + H(p,\bar{p},\theta),\end{aligned} \tag{4.17}$$

where,

$$H(p,\bar{p},\theta) = H_{20}(\theta)\frac{p^2}{2} + H_{11}(\theta)p\bar{p} + H_{02}(\theta)\frac{\bar{p}^2}{2} + H_{21}(\theta)\frac{p^2\bar{p}}{2} + \cdots. \tag{4.18}$$

According to Eq (4.17) and (4.18), we can obtain

$$\begin{aligned}(A - 2i\omega_k\bar{\tau})W_{20}(\theta) &= -H_{20}(\theta), \\ AW_{11}(\theta) &= -H_{11}(\theta), \\ (A + 2i\omega_k\bar{\tau})W_{02}(\theta) &= -H_{02}(\theta).\end{aligned} \tag{4.19}$$

According to Eq (4.13), we can obtain

$$\begin{aligned}U_t(\theta) =& W(t,\theta) + 2Re\left\{p(t)q(\theta)\right\} \\ =& W_{20}(\theta)\frac{p^2}{2} + W_{11}(\theta)p\bar{p} + W_{02}(\theta)\frac{\bar{p}^2}{2} \\ &+ (1,q_1,q_2)^{\mathrm{T}}e^{i\omega_k\bar{\tau}\theta}p + (1,\bar{q}_1,\bar{q}_2)^{\mathrm{T}}e^{-i\omega_k\bar{\tau}\theta}\bar{p} + \cdots.\end{aligned} \tag{4.20}$$

Furthermore, we have

$$\begin{aligned}g(p,\bar{p}) =& \bar{q}^*(0)F(0,U_t) = \bar{D}\bar{\tau}[F_1(U_t) + \bar{q}_1^*F_2(U_t) + \bar{q}_2^*F_3(U_t)] \\ =& \frac{p^2}{2}[2\bar{D}\bar{\tau}(k_{11} + k_{21}\bar{q}_1^* + k_{31}\bar{q}_2^*)] + p\bar{p}[\bar{D}\bar{\tau}(k_{12} + k_{22}\bar{q}_1^* + k_{32}\bar{q}_2^*)] \\ &+ \frac{\bar{p}^2}{2}[2\bar{D}\bar{\tau}(k_{13} + k_{23}\bar{q}_1^* + k_{33}\bar{q}_2^*)] + \frac{p^2\bar{p}}{2}[2\bar{D}\bar{\tau}(k_{14} + k_{24}\bar{q}_1^* + k_{34}\bar{q}_2^*)],\end{aligned} \tag{4.21}$$

for the meanings of the remaining parameters in the Eq (4.21), see Eq (7.2) in the Appendix.

Following the analytical procedure [22,23], we can derive four key parameters which determine the properties of Hopf bifurcation,

$$\begin{aligned}g_{20} &= 2\bar{D}\bar{\tau}(k_{11} + \bar{q}_1^*k_{21} + \bar{q}_2^*k_{31}), g_{11} = \bar{D}\bar{\tau}(k_{12} + \bar{q}_1^*k_{22} + \bar{q}_2^*k_{32}), \\ g_{02} &= 2\bar{D}\bar{\tau}(k_{13} + \bar{q}_1^*k_{23} + \bar{q}_2^*k_{33}), g_{21} = 2\bar{D}\bar{\tau}(k_{14} + \bar{q}_1^*k_{24} + \bar{q}_2^*k_{34}).\end{aligned} \tag{4.22}$$

Since the expression of g_{21} involves both $W_{20}(\theta)$ and $W_{11}(\theta)$, it is necessary to compute these terms explicitly. When $\theta \in [-1,0)$, according to Eq (4.17), we obtain

$$H(p,\bar{p},\theta) = -2Re\left\{\bar{q}^*(0)F_0(p,\bar{p})q(\theta)\right\} = -2Re\left\{g(p,\bar{p})q(\theta)\right\} = -g(p,\bar{p})q(\theta) - \bar{g}(p,\bar{p})\bar{q}(\theta). \tag{4.23}$$

Comparing the coefficients of Eq (4.18) and (4.23), we obtain

$$H_{20}(\theta) = -g_{20}q(\theta) - \bar{g}_{02}\bar{q}(\theta), H_{11}(\theta) = -g_{11}q(\theta) - \bar{g}_{11}\bar{q}(\theta). \tag{4.24}$$

According to Eq (4.19), we get

$$\dot{W}_{20}(\theta) = 2i\omega_k\bar{\tau}W_{20}(\theta) + g_{20}q(\theta) + \bar{g}_{02}\bar{q}(\theta), \dot{W}_{11}(\theta) = g_{11}q(\theta) + \bar{g}_{11}\bar{q}(\theta). \tag{4.25}$$

To solve Eq (4.25), we obtain

$$\begin{aligned} W_{20}(\theta) &= \frac{ig_{20}q(0)}{\omega_k\bar{\tau}}e^{i\omega_k\bar{\tau}\theta} + \frac{i\bar{g}_{02}\bar{q}(0)}{3\omega_k\bar{\tau}}e^{-i\omega_k\bar{\tau}\theta} + E_1e^{2i\omega_k\bar{\tau}\theta}, \\ W_{11}(\theta) &= -\frac{ig_{11}q(0)}{\omega_k\bar{\tau}}e^{i\omega_k\bar{\tau}\theta} + \frac{i\bar{g}_{11}\bar{q}(0)}{\omega_k\bar{\tau}}e^{-i\omega_k\bar{\tau}\theta} + E_2, \end{aligned} \tag{4.26}$$

where $E_i = (E_i^{(1)}, E_i^{(2)}, E_i^{(3)}) \in R^3 (i = 1, 2)$ are constant vectors.

When $\theta = 0$, using Eq (4.17), we have

$$H(p, \bar{p}, 0) = -2Re\{\bar{q}^*(0)F_0(p, \bar{p})q(0)\} + F_0.$$

According to Eq (4.18), we get

$$\begin{aligned} H_{20}(0) &= -g_{20}q(0) - \bar{g}_{02}\bar{q}(0) + 2\bar{\tau}\begin{pmatrix} k_{11} \\ k_{21} \\ k_{31} \end{pmatrix}, \\ H_{11}(0) &= -g_{11}q(0) - \bar{g}_{11}\bar{q}(0) + \bar{\tau}\begin{pmatrix} k_{12} \\ k_{22} \\ k_{32} \end{pmatrix}. \end{aligned} \tag{4.27}$$

From the definition of $A(0)$ and Eq (4.19), we can derive

$$\int_{-1}^{0} d\eta(\theta)W_{20}(\theta) = 2i\omega_k\bar{\tau}W_{20} - H_{20}(0), \int_{-1}^{0} d\eta(\theta)W_{11}(\theta) = -H_{11}(0), \tag{4.28}$$

where $\eta(\theta) = \eta(\theta, 0)$.

According to Eq (4.9), (4.11), and (4.28), we get

$$\begin{aligned} &\bar{\tau}L_1W_{20}(0) + \bar{\tau}L_2W_{20}(-1) = 2i\omega_k\bar{\tau} - H_{20}(0), \\ &\bar{\tau}L_1W_{11}(0) + \bar{\tau}L_2W_{11}(-1) = H_{11}(0). \end{aligned} \tag{4.29}$$

Substituting Eq (4.26) and (4.27) into Eq (4.29), we obtain

$$\begin{aligned} E_1 &= 2\begin{pmatrix} 2i\omega_k - a_{11} & -a_{12} & -a_{13} \\ -a_{21} & 2i\omega_k & -a_{23} \\ -b_{31}e^{-2i\omega_k\bar{\tau}} & -b_{32}e^{-2i\omega_k\bar{\tau}} & 2i\omega_k - a_{33} - b_{33}e^{-2i\omega_k\bar{\tau}} \end{pmatrix}^{-1}\begin{pmatrix} k_{11} \\ k_{21} \\ k_{31} \end{pmatrix}, \\ E_2 &= \begin{pmatrix} -a_{11} & -a_{12} & -a_{13} \\ -a_{21} & 0 & -a_{23} \\ -b_{31} & -b_{32} & -a_{33} - b_{33} \end{pmatrix}^{-1}\begin{pmatrix} k_{12} \\ k_{22} \\ k_{32} \end{pmatrix}. \end{aligned}$$

Therefore, all coefficients g_{ij} can be explicitly determined. Furthermore, we derive

$$\begin{cases} c_1(0) = \frac{i}{2\omega_k\bar{\tau}}(g_{20}g_{11} - 2|g_{11}|^2 - \frac{|g_{02}|^2}{3}) + \frac{g_{21}}{2}, \\ \mu_1 = -\frac{Re\{c_1(0)\}}{Re\{\lambda'(\bar{\tau})\}}, \\ \mu_2 = 2Re\{c_1(0)\}, \\ T_1 = -\frac{Im\{c_1(0)\}+\mu_1 Im\{\lambda'(\bar{\tau})\}}{\omega_k\bar{\tau}}. \end{cases} \tag{4.30}$$

At $\tau = \bar{\tau}$, Eq (4.30) governs the direction of the Hopf bifurcation and the stability properties of the periodic solutions emerging on the center manifold.

Theorem 4.3. *From Eq (4.30), we obtain the following results:*

(i) The sign of μ_1 dictates the direction of Hopf bifurcation: A positive (negative) μ_1 indicates a supercritical (subcritical) bifurcation, with periodic solutions emerging for $\tau > \bar{\tau}$ in the supercritical case.

(ii) The stability of the bifurcating periodic solutions is governed by μ_2: When $\mu_2 < 0$ (> 0), the solutions are stable (unstable).

(iii) The period of these solutions is characterized by T_1: A positive (negative) T_1 implies an increase (decrease) in the period.

5. The MMS and suppression of oscillations

5.1. Hopf bifurcation analysis via MMS

The multiple time scales method [24–27] is commonly used to analyze phenomena spanning different temporal and spatial scales. Here, we implement this approach for model (4.1).

From the preceding analysis, the system admits a unique positive equilibrium $E^*(S^*, I^*, P^*)$. To begin, we linearize model (4.1) around this equilibrium by introducing the perturbations $U_1(t) = S(t) - S^*, U_2(t) = I(t) - I^*, U_3(t) = P(t) - P^*$. Thus, we obtain a differential equation about the variable U

$$\dot{U} = F(U, U_\tau), \tag{5.1}$$

where $U = (S, I, P)^{\mathrm{T}} = (U_1, U_2, U_3)^{\mathrm{T}}$, and $U_\tau = U(t - \tau)$.

Following the multiple time scales method, we first introduce the new time scales and the corresponding time derivatives as

$$T_k = \epsilon^k t, \frac{\mathrm{d}}{\mathrm{d}t} = \sum_{k=0}^{\infty} \epsilon^k D_k, \tag{5.2}$$

where $D_k = \frac{\partial}{\partial T_k}$ for $k \in \mathbb{N} \cup \{0\}$. To study the Hopf bifurcation by means of the multiple scales technique, we perturb the bifurcation parameter of system (5.1) around its critical threshold by setting $\tau = \bar{\tau} + \epsilon\tau_\epsilon$, where ϵ is a small positive quantity. Following the approach in [24], the solution to model (5.1) is sought in the form,

$$U(t) = U(T_0, T_1, T_2, \cdots) = \sum_{k=1}^{\infty} \epsilon^k U_k(T_0, T_1, T_2, \cdots). \tag{5.3}$$

Moreover, by employing multiple time scales, we can obtain an asymptotic expansion for the delayed solutions of model (5.1), which can be expressed as

$$U_\tau = \sum_{k=1}^{\infty} \epsilon^k U_k(T_0 - \bar{\tau}, T_1 - \epsilon\bar{\tau}, T_2 - \epsilon^2\bar{\tau}). \tag{5.4}$$

Substituting Eq (5.3) and Eq (5.4) into model (5.1), and using multivariate Taylor expansion, we collect the terms according to powers of ϵ. Beginning with the lowest order of ϵ, we obtain

$$D_0U_1 - F_UU_1 - F_{U_\tau}U_{1_\tau} = 0, \tag{5.5}$$

where $F_U = \frac{\partial F}{\partial U}, F_{U_\tau} = \frac{\partial F}{\partial U_\tau}$. Furthermore, we assume that the solution of Eq (5.5) can be written in the following form

$$\begin{aligned} U_1 &= M_1 \sin(\omega T_0) + N_1 \cos(\omega T_0), \\ U_{1_\tau} &= M_1 \sin(\omega(T_0 - \bar{\tau})) + N_1 \cos(\omega(T_0 - \bar{\tau})), \end{aligned} \tag{5.6}$$

where $M_1 = (M_{11}(T_1, T_2, \cdots), M_{12}(T_1, T_2, \cdots), M_{13}(T_1, T_2, \cdots))^{\mathrm{T}}$, $N_1 = (N_{11}(T_1, T_2, \cdots)$, $N_{12}(T_1, T_2, \cdots)$, and $N_{13}(T_1, T_2, \cdots))^{\mathrm{T}}$. For conciseness, we express the above equations as

$$M_{1n}(T_1, T_2, \cdots) = M_{1n}, N_{1n}(T_1, T_2, \cdots) = N_{1n}, n = 1, 2, 3.$$

Substituting Eq (5.6) into Eq (5.5), we get

$$\begin{aligned} &\omega M_1 \cos(\omega T_0) - \omega N_1 \sin(\omega T_0) - F_U M_1 \sin(\omega T_0) - F_U N_1 \cos(\omega T_0) \\ &- F_{U_\tau} M_1 \sin(\omega T_0 - \omega\bar{\tau}) - F_{U_\tau} N_1 \cos(\omega T_0 - \omega\bar{\tau}) = 0. \end{aligned}$$

Then we derive that M_{12}, M_{13}, N_{12}, and N_{13} can be represented by M_{11} and N_{11}, respectively. Consequently, we arrive at the following system of linear equations:

$$M_{1,j} = \alpha_{1,j}(M_{1,1}, N_{1,1}), N_{1,j} = \beta_{1,j}(M_{1,1}, N_{1,1}), j = 2, 3. \tag{5.7}$$

Similar to Eq (5.2), denote $\frac{\mathrm{d}}{\mathrm{d}T_k}$ by D_k for $k = 0, 1, \cdots$. From Eq (5.7), we have

$$D_1M_{1,i} = \alpha_{1,i}(D_1M_{1,1}, D_1N_{1,1}), D_1N_{1,i} = \beta_{1,i}(D_1M_{1,1}, D_1N_{1,1}), i = 2, 3.$$

Substituting (5.3) and (5.4) into model (5.1) and applying Taylor expansion, we obtain the following equation at order ϵ^2:

$$D_0U_2(T_0, T_1, T_2, \cdots) - F_UU_2(T_0, T_1, T_2, \cdots) - F_{U_\tau}U_{2\tau}(T_0 - \bar{\tau}, T_1, T_2, \cdots) = g_1(U_1, U_{1\tau}),$$

where,

$$\begin{aligned} g_1(U_1, U_{1\tau}) =& \frac{1}{2}F_{UU}U_1^2 + \frac{1}{2}F_{U_\tau U_\tau}U_{1\tau}^2 + F_{UU_\tau}U_1U_{1\tau} - F_{U_\tau}(\tau_\epsilon D_0U_{1\tau} + \bar{\tau}D_1U_{1\tau}) - D_1U_1 \\ =& \frac{1}{2}F_{UU}(\frac{M_1^2(1-\cos(2\omega T_0))}{2} + \frac{N_1^2(1+\cos(2\omega T_0))}{2} \\ &+ M_1N_1\sin(2\omega T_0)) + \frac{1}{2}F_{U_\tau U_\tau}(M_1N_1\sin(2(\omega T_0 - \omega\bar{\tau})) \\ &+ \frac{M_1^2(1-\cos(2(\omega T_0 - \omega\bar{\tau})))}{2} + \frac{N_1^2(1+\cos(2(\omega T_0 - \omega\bar{\tau})))}{2}) \\ &+ F_{UU_\tau}(M_1\sin(\omega T_0) + N_1\cos(\omega T_0))(M_1\sin(\omega(T_0 - \bar{\tau})) \\ &+ N_1\cos(\omega(T_0 - \bar{\tau}))) - F_{U_\tau}(\tau_\epsilon\omega(M_1\cos(\omega(T_0 - \bar{\tau})) \\ &- N_1\sin(\omega(T_0 - \bar{\tau}))) + \bar{\tau}(D_1M_1\sin(\omega(T_0 - \bar{\tau})) \\ &+ D_1N_1\cos(\omega(T_0 - \bar{\tau})))) - D_1M_1\sin(\omega T_0) - D_1N_1\cos(\omega T_0). \end{aligned} \tag{5.8}$$

For the equation to be solvable, all secular terms containing $\sin(\omega T_0)$ and $\cos(\omega T_0)$ must be removed from the asymptotic expansion. That is, let the coefficients of $\sin(\omega T_0)$ and $\cos(\omega T_0)$ in Eq (5.8) be zero. From Eq (5.8), we derive the following equations

$$\begin{cases} -F_{U_\tau}\tau_\epsilon\omega M_1\sin(\omega\bar{\tau}) + F_{U_\tau}\tau_\epsilon\omega N_1\cos(\omega\bar{\tau}) - F_{U_\tau}\bar{\tau}D_1N_1\sin(\omega\bar{\tau}) - F_{U_\tau}\bar{\tau}D_1M_1\cos(\omega\bar{\tau}) = D_1M_1, \\ -F_{U_\tau}\tau_\epsilon\omega N_1\sin(\omega\bar{\tau}) - F_{U_\tau}\tau_\epsilon\omega M_1\cos(\omega\bar{\tau}) + F_{U_\tau}\bar{\tau}D_1M_1\sin(\omega\bar{\tau}) - F_{U_\tau}\bar{\tau}D_1N_1\cos(\omega\bar{\tau}) = D_1N_1. \end{cases}$$

After removing the asymptotic oscillatory terms, Eq (5.8) can be rewritten in the following form:

$$\begin{aligned} & D_0U_2 - F_UU_2 - F_{U_\tau}U_{2\tau} \\ =& \frac{1}{2}F_{UU}(\frac{M_1^2+N_1^2}{2} + \frac{N_1^2-M_1^2}{2}\cos(2\omega T_0) + M_1N_1\sin(2\omega T_0)) \\ &+ \frac{1}{2}F_{U_\tau U_\tau}(\frac{M_1^2+N_1^2}{2} + \frac{N_1^2-M_1^2}{2}\cos(2\omega(T_0 - \bar{\tau})) + M_1N_1\sin(2\omega(T_0 - \bar{\tau}))) \\ &+ F_{UU_\tau}M_1\sin(\omega T_0)(M_1\sin(\omega(T_0 - \bar{\tau})) + N_1\cos(\omega(T_0 - \bar{\tau}))) \\ &+ F_{UU_\tau}N_1\cos(\omega T_0)(M_1\sin(\omega(T_0 - \bar{\tau})) + N_1\cos(\omega(T_0 - \bar{\tau}))). \end{aligned} \tag{5.9}$$

To solve Eq (5.9) while satisfying the solvability conditions, the solution of Eq (5.9) is

$$\begin{aligned} U_2 &= M_2\sin(2\omega T_0) + N_2\cos(2\omega T_0) + O_2, \\ U_{2\tau} &= M_2\sin(2\omega(T_0 - \bar{\tau})) + N_2\cos(2\omega(T_0 - \bar{\tau})) + O_2, \end{aligned}$$

where $U_2 = U_2(T_0, T_1, T_2, \cdots)$, $M_2 = M_2(T_1, T_2, T_3, \cdots)$, $N_2 = N_2(T_1, T_2, T_3, \cdots)$, $O_2 = O_2(T_1, T_2, T_3, \cdots)$, and O_2 can be denoted by M_1 and N_1, namely

$$O_2 = -\frac{1}{4}\frac{F_{UU} + F_{U_\tau U_\tau}}{F_U + F_{U_\tau}}(M_1^2 + N_1^2).$$

Proceeding analogously to the cases of ϵ and ϵ^2, we now gather the ϵ^3 order terms from Eq (5.1),

$$D_0U_3(T_0, T_1, \cdots) - F_UU_3(T_0, T_1, \cdots) - F_{U_\tau}U_{3\tau}(T_0 - \bar{\tau}, T_1, \cdots) = g_2(U_i, U_{i\tau}), i = 1, 2.$$

For the meanings of the remaining parameters, see Eq.(7.3) in the Appendix, where $D_{00} = \frac{\partial^2}{\partial T_0^2}$, $D_{01} = \frac{\partial^2}{\partial T_0 T_1}$, and $D_{11} = \frac{\partial^2}{\partial T_1^2}$. The term g_2 generally comprises the Taylor series expansion of the delayed state U_τ, nonlinear interactions between system states U_1 and U_2, and higher-order temporal derivative terms.

Consistent with the previous order analysis, we must eliminate secular terms containing asymptotic oscillations to satisfy the solvability condition. After calculation, we obtain that the expressions of D_2M_{11} and D_2N_{11} are related to M_{11} and N_{11} at ϵ^3, which are too intricate to be presented here. Finally, reverting to the original time scale, we arrive at

$$\begin{cases} \frac{\mathrm{d}M_{11}}{\mathrm{d}t} = \epsilon D_1 M_{11} + \epsilon^2 D_2 M_{11} + \cdots, \\ \frac{\mathrm{d}N_{11}}{\mathrm{d}t} = \epsilon D_1 N_{11} + \epsilon^2 D_2 N_{11} + \cdots. \end{cases} \tag{5.10}$$

To carry out the normal form analysis, we introduce the following polar coordinate transformations for model (5.10)

$$M_{11} = R(t)\cos(\varphi t), N_{11} = R(t)\sin(\varphi t).$$

Consequently, when $\tau = \bar{\tau} + \epsilon\tau_\epsilon$, the amplitude-frequency equation for model (5.10) takes the form

$$\begin{cases} \frac{\mathrm{d}R}{\mathrm{d}t} = P_1(\epsilon, \tau_\epsilon)R(t) + P_3(\epsilon, \tau_\epsilon)R^3(t) + O(\epsilon^3), \\ \frac{\mathrm{d}\varphi}{\mathrm{d}t} = P_0(\epsilon, \tau_\epsilon) + P_2(\epsilon, \tau_\epsilon)R^2(t) + O(\epsilon^3). \end{cases} \tag{5.11}$$

5.2. Oscillation suppression analysis based on periodic time delay

Bifurcation theory, describes qualitative changes in system behavior under parameter variation. These transitions may induce instability, generate limit cycles, or precipitate chaotic dynamics [28,29]. Bifurcation control has emerged as a key research focusing on improving system performance metrics (reliability, stability) while mitigating implementation challenges in practical scenarios. Conventional bifurcation control methodologies include parameter tuning [29,30], feedback control [31,32], delayed feedback control [33, 34], and hybrid control [35, 36].

We now proceed to analyze model (4.1). As demonstrated in other studies, the time delay in this model can induce periodic solutions through Hopf bifurcation. Furthermore, we set $\tau_m = \bar{\tau} + \epsilon\tau_\epsilon$, where $\epsilon\tau_\epsilon > 0$. Thus, we propose implementing a perturbation control strategy through time-varying delay modulation with the objective of oscillation suppression [25, 37]. Specifically, let

$$\tau(t) = \tau_m + L\sin(\Omega t), \tag{5.12}$$

where L and Ω denote the amplitude and frequency of the perturbation, respectively. Assume that L and Ω are small, so that $L\sin(\Omega t)$ can be considered as a perturbation to τ_m. Thus, the method of multiple scales proves applicable for investigating time-varying delay systems. Substituting Eq (5.12) into system (5.1), we obtain

$$\dot{U}(t) = F(U, U(t - \tau(t))). \tag{5.13}$$

To obtain the amplitude-frequency equation for model (5.10) under the condition $\tau(t) = \bar{\tau} + \epsilon\tau_\epsilon + L\sin(\Omega t)$, a re-scaling procedure is performed, where $\epsilon R(t)$ is replaced with $R(t)$. By applying the

method outlined in Subsection 4.2, this yields the amplitude-frequency equation given by

$$\begin{cases} \frac{\mathrm{d}R}{\mathrm{d}t} = P_1(t)R(t) + P_3(t)R^3(t), \\ \frac{\mathrm{d}\varphi}{\mathrm{d}t} = P_0(t) + P_2(t)R^2(t), \end{cases} \tag{5.14}$$

where $P_1(t) = q_0 + q_{11}\sin(\Omega t) + q_{12}\cos(\Omega t)$, $P_0(t) = r_0 + r_{11}\sin(\Omega t) + r_{12}\cos(\Omega t)$, $q_0 = q_0(\epsilon\tau_\epsilon, L, \Omega)$, $q_{11} = q_{11}(\epsilon\tau_\epsilon, L, \Omega)$, $q_{12} = q_{12}(\epsilon\tau_\epsilon, L, \Omega)$, $r_0 = r_0(\epsilon\tau_\epsilon, L, \Omega)$, $r_{11} = r_{11}(\epsilon\tau_\epsilon, L, \Omega)$, and $r_{12} = r_{12}(\epsilon\tau_\epsilon, L, \Omega)$. $P_2(t)$ and $P_3(t)$ are functions of ϵ.

Since the first equation in (5.14) exclusively governs $R(t)$, whereas the second equation is $R(t)$-dependent, we focus on the first equation,

$$\frac{\mathrm{d}R}{\mathrm{d}t} = P_1(t)R(t) + P_3(t)R^3(t). \tag{5.15}$$

We observe that Eq (5.15) constitutes a variable-coefficient Bernoulli equation, whose solution may be obtained through application of the following lemma.

Lemma 3. *The solution to Eq (5.15) can be written analytically in the following form*

$$R(t) = \frac{Ce^{\int_0^t P_1(s)ds}}{\sqrt{1 - 2C^2\int_0^t P_3(s_2)e^{2\int_0^{s_2} P_1(s_1)ds_1}ds_2}}, \tag{5.16}$$

with C representing the initial condition.

Remarkably, the asymptotic decay of solutions to Eq (5.15) directly reflects the attenuation characteristics of bursting solutions in the original model (5.1). In this subsection, we derive a sufficient condition for the decay of solutions to Eq (5.15), leading to the following theorem.

Theorem 5.1. *A sufficient condition for the decay of solutions in model (5.14) is given by $q_0 < 0$, where q_0 depends on the parameters $\epsilon\tau_\epsilon$, L, and Ω.*

Proof. Since $C > 0$ in Eq (5.16), we can rewrite Eq (5.16) as:

$$R(t) = \frac{1}{\sqrt{C^{-2}e^{-2\int_0^t P_1(s)ds} - 2e^{-2\int_0^t P_1(s)ds}\int_0^t P_3(s_2)e^{2\int_0^{s_2} P_1(s_1)ds_1}ds_2}}, \tag{5.17}$$

By employing Fourier series expansion and incorporating Eq (5.17), we obtain

$$\bar{C}e^{-2q_0(t)}Y_1(t) + Y_2(t) = -2e^{-2\int_0^t P_1(s)ds}\int_0^t P_3(s_2)e^{2\int_0^{s_2} P_1(s_1)ds_1}ds_2 + \bar{C}e^{-2\int_0^t P_1(s)ds}, \tag{5.18}$$

In this expression, $\bar{C}$ is defined as C^{-2}, and both $Y_1(t)$ and $Y_2(t)$ are periodic, having period $\frac{2\pi}{\Omega}$. Thus, $\bar{C} > 0$ holds, and the asymptotic behavior of $\tilde{v}(t) = \bar{C}e^{-2q_0(t)}Y_1(t) + Y_2(t)$ is dictated by the sign of $q_0(t)$. If $q_0(t) \geq 0$, the term $\bar{C}e^{-2q_0(t)}Y_1(t)$ decays exponentially; consequently, the long-term dynamics of $\tilde{v}(t)$ are dominated by $Y_2(t)$, which induces periodic oscillations in $R(t)$. Conversely, if $q_0(t) < 0$, then $\tilde{v}(t)$ increases exponentially, which leads to the exponential decay of oscillations in $R(t) = \frac{1}{\sqrt{\tilde{v}(t)}}$ over time. In summary, when the delay perturbation parameters satisfy specific conditions guaranteeing $q_0(t) < 0$, the oscillatory behavior of model (1.1) becomes controllable. Consequently, the critical stability boundary can be determined by solving equation $q_0(\epsilon\tau_\epsilon, L, \Omega) = 0$.

6. Numerical simulations

In this section, we employ the parameter values to numerically validate the theoretical predictions and provide corresponding biological interpretations. Using the parameter values listed in Table 1, we find that there exists only one trivial equilibrium, namely $E_1(0, 0, 0)$, the susceptible-prey-only equilibrium $E_2(39.2, 0, 0)$, the predator-only equilibrium $E_3(0, 0, 3.2879)$, the predator-free equilibrium $E_4(0.3000, 3.2119, 0)$, the disease-free equilibrium $E_5(37.9527, 0, 4.4777)$, and the positive equilibrium $E^*(16.2569, 9.7103, 6.0314)$.

For the non-delayed model (2.1), the predator-only equilibrium E_3 exhibits the local asymptotic stability, as established by Theorem 3.3 (see Figure 2(a), indicating that when the target prey population goes extinct, predators can persist by relying on additional foods-a pattern well-aligned with the ecological characteristics of large carnivores (i.e., our generalist predators) in natural systems. The predator-free equilibrium E_4, the disease-free equilibrium E_5, and the positive equilibrium E^* exhibit local asymptotic stability, as established by Theorem 3.4, Theorem 3.5, and Theorem 3.6, respectively (see Figure 2(b), Figure 2(c), and Figure 4). Consequently, susceptible prey, infected prey, and predator populations exhibit stable coexistence dynamics.

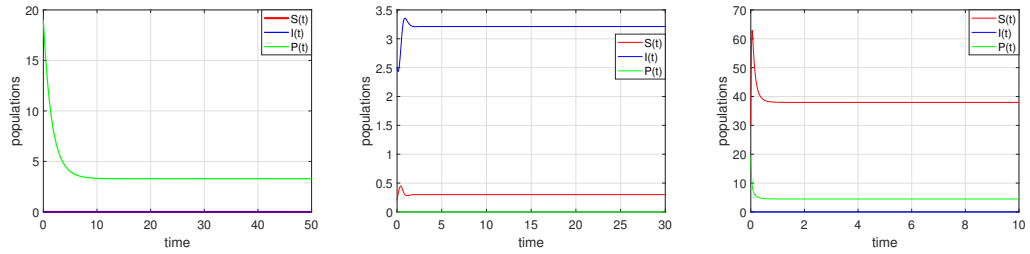

(a) (b) (c)

Figure 2. Model (2.1) is locally asymptotically stable around the equilibriums. (a) The predator-only equilibrium E_3, (b) the predator-free equilibrium E_4, and (c) the disease-free equilibrium E_5.

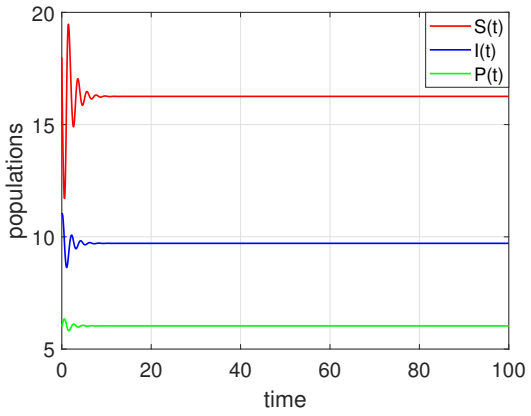

Figure 3. Model (2.1) is locally asymptotically stable around the positive equilibrium E^*.

Theorem 3.7 establishes that E^* is globally asymptotically stable for the specified parameters

(Figure 4), indicating that model (2.1) converges to steady-state population levels that are independent of initial conditions. In other words, irrespective of the starting densities, the predator and prey populations will converge to constant levels corresponding to the positive equilibrium of the model.

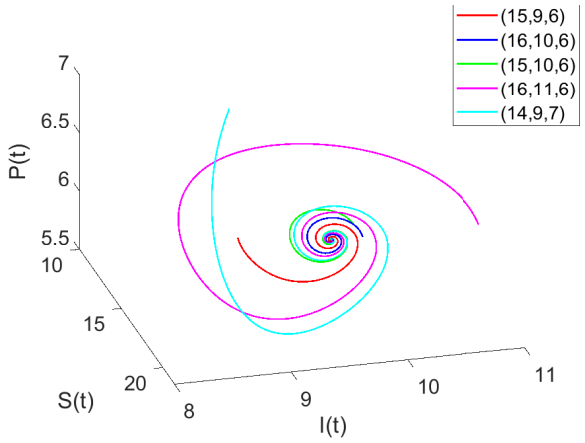

Figure 4. Model (2.1) is globally asymptotically stable at the positive equilibrium E^*.

For the time-varying delay model (1.1), we maintain the parameter values specified in Table 1, under which the positive equilibrium E^* persists unchanged from the non-delayed case. First, when gestation delay is chosen as $\tau(t) = \frac{|\sin(t^3)|}{1+t^2}$, Figure 5 provides numerical verification of the global asymptotic stability of model (1.1) at the positive equilibrium. In contrast, for $\tau(t) = |\sin(t^2)| + 10$, the solution of model (1.1) is found to be unstable. Furthermore, when $\tau(t) = |\sin(t^2)| + 10$, susceptible prey, infected prey, and predator populations exhibit sustained periodic oscillations, as demonstrated in Figure 6. Through combined analytical investigation and numerical simulations, we demonstrate that time-varying delay serves as a crucial bifurcation parameter governing the stability of model (1.1). When $\tau(t)$ is sufficiently small, model (1.1) remains stable. This finding suggests potential control strategies for population stabilization through deliberate manipulation of time-varying delay parameters. Conversely, sufficiently large time-varying delays can destabilize the model, potentially inducing chaotic dynamics. This underscores the critical importance of early population control measures for maintaining ecosystem stability, as well as controlling the transmission and suppression of the disease.

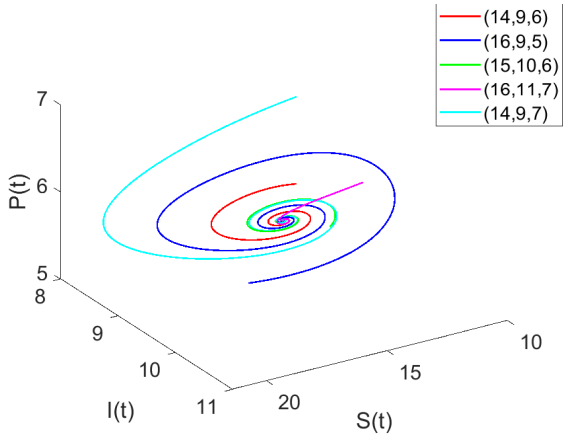

Figure 5. When $\tau(t) = \frac{|\sin(t^3)|}{1+t^2}$, model (1.1) is globally asymptotically stable at E^*.

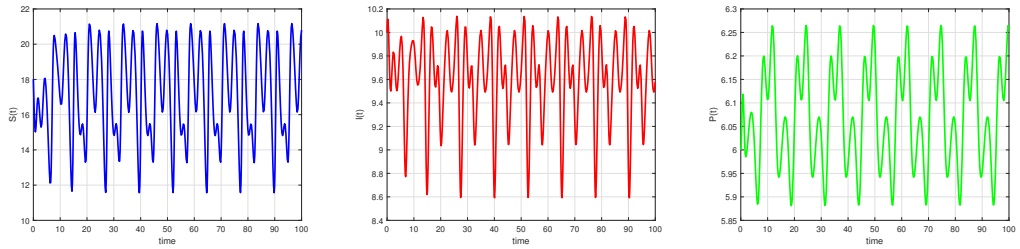

(a) (b) (c)

Figure 6. When $\tau(t) = |\sin(t^2)| + 10$, the positive equilibrium E^* of model (1.1) is unstable. (a) $S(t)$, (b) $I(t)$, and (c) $P(t)$.

For delayed model (4.1), model has the same positive equilibrium $E^*(16.2569, 9.7103, 6.0314)$. We can calculate that $\bar{\tau} = 0.2248$. Our analysis reveals that model (4.1) undergoes a Hopf bifurcation at equilibrium E^* when $\tau = \bar{\tau} = 0.2248$, giving rise to periodic solutions as visualized in Figure 7. As established in Theorem 4.2, the equilibrium E^* is locally asymptotically stable for $\tau = 0.2 < \bar{\tau}$ (see Figure 8), whereas it becomes unstable when $\tau = 0.24 > \bar{\tau}$ (see Figure 9). From an ecological perspective, when the gestation delay remains below the critical value, the prey and predator populations can persist together indefinitely. However, once the delay exceeds this critical value, the susceptible prey, infected prey, and predator coexist at positive densities, although their populations now undergo periodic oscillations over time.

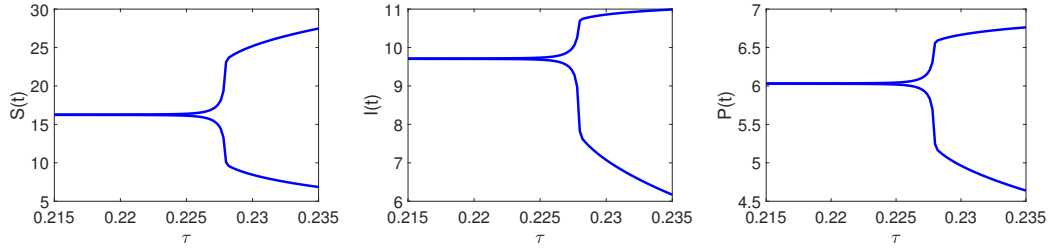

Figure 7. Bifurcation diagrams of model (4.1) by taking τ as bifurcation parameter. (a) $S(t)$, (b) $I(t)$, and (c) $P(t)$.

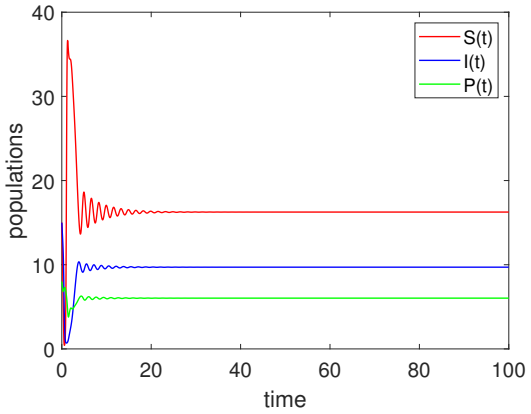

Figure 8. When $\tau = 0.2 < 0.2248$, the positive equilibrium E^* of model (4.1) is locally asymptotically stable.

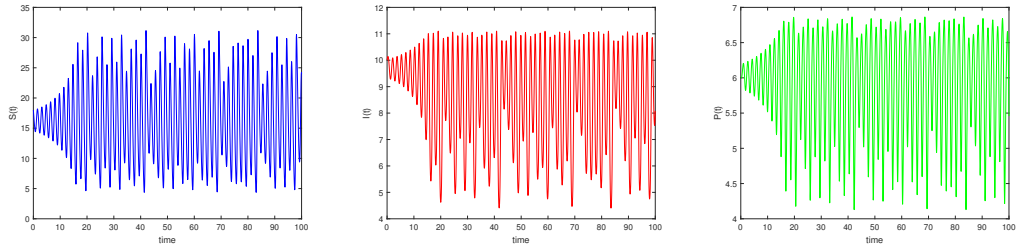

Figure 9. When $\tau = 0.24 > 0.2248$, the positive equilibrium E^* of model (4.1) is unstable. (a) $S(t)$, (b) $I(t)$, and (c) $P(t)$.

We also consider the impact of additional food on equilibriums for model (1.1). First, setting $\tau(t) = 0.1$ and keeping all other parameter values as in Table 1 except for η and η_0, we observe that as η increases and η_0 decreases, the values of equilibrium $E^*(S^*, I^*, P^*)$ rise (see Figure 10 (a), (b), (c)). These results indicate that when the predator's growth rate from additional food (η) increases, the population sizes of susceptible prey, infected prey, and predators increase; conversely, when the

predator's reliance on additional food (η_0) increases, the three population sizes decrease. This suggests that conservation measures, which enhance the availability of additional food for predators while preventing excessive dependence on it, can promote richer species diversity and help maintain high level stability in the ecosystem.

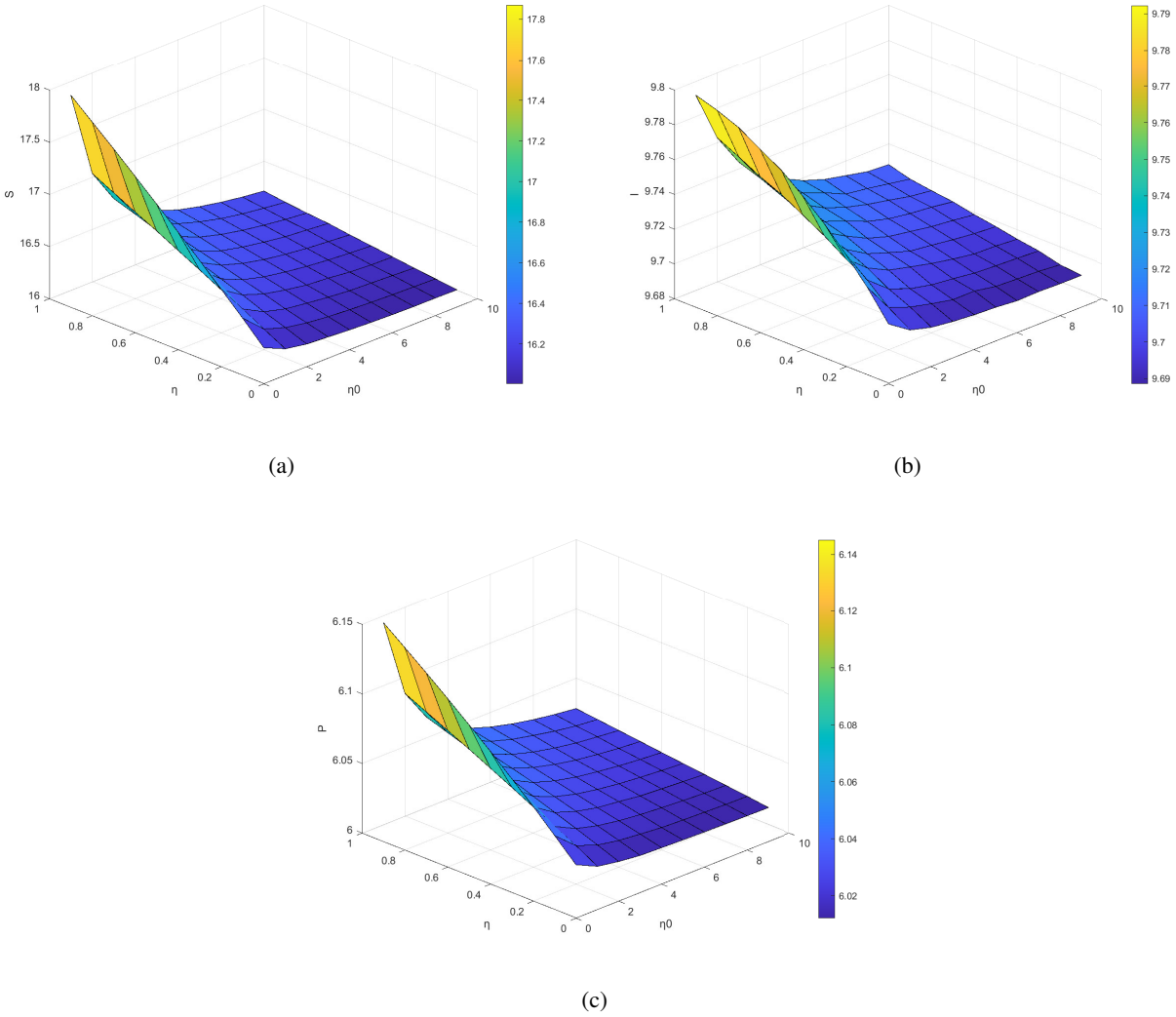

(a) (b)

(c)

Figure 10. Effect of additional food coefficients η and η_0 on the positive equilibrium E^* when $\tau(t) = 0.1$. (a)S^*, (b) I^*, and (c) P^*.

Furthermore, nonlinear prey refuge also significantly affects the positive equilibrium of model (1.1). Again, setting $\tau(t) = 0.1$ and keeping all other parameters as in Table 1 except for δ_1 and δ_2, we find that susceptible prey vary irregularly with changes in δ_1 and δ_2. Infected prey become extinct when both δ_1 and δ_2 take very small values, whereas the predator population reaches its maximum when the refuge coefficients are very small or zero (see Figure 11(a), (b), (c)). These results indicate that appropriately controlling the values of refuge coefficients can reduce or eliminate disease transmission. In ecosystem conservation, excessive human intervention, particularly the imposition of excessively high refuge coefficients, may undermine system stability and lead to species extinction. Conversely,

maintaining relatively low refuge coefficients helps promote ecological stability.

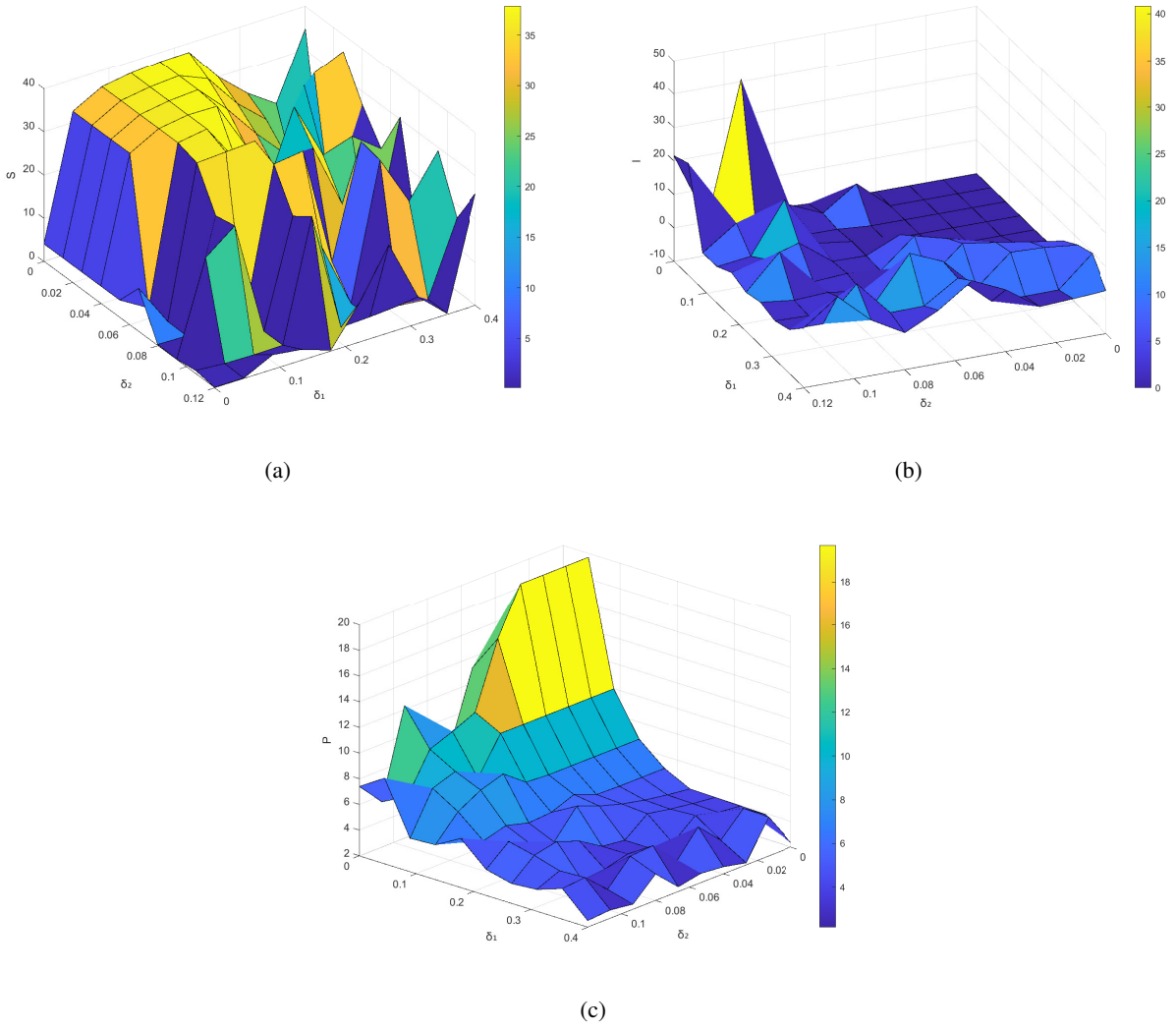

(a) (b)

(c)

Figure 11. Effect of nonlinear prey refuge coefficients δ_1 and δ_2 on the equilibriums in model (1.1) when $\tau(t) = 0.1$. (a) S^*, (b)I^*, and (c)P^*.

By applying the multiple time scales method developed in Subsection 5.1, we derive the governing amplitude-frequency equation

$$\begin{cases} \frac{dR}{dt} = (24.3344\epsilon\tau_\epsilon - 24.1186\epsilon^2\tau_\epsilon^2)R(t) - 5.5301\epsilon^2R^3(t) + O(\epsilon^3), \\ \frac{d\phi}{dt} = -45.5468\epsilon\tau_\epsilon + 52.3654\epsilon^2\tau_\epsilon^2 + 3.8648\epsilon^2R^2(t) + O(\epsilon^3). \end{cases} \tag{6.1}$$

Next, multiplying the first equation of system (6.1) throughout by ϵ gives

$$\epsilon\frac{dR}{dt} = (24.3344\epsilon\tau_\epsilon - 24.1186\epsilon^2\tau_\epsilon^2)(\epsilon R(t)) - 5.5301(\epsilon R(t))^3. \tag{6.2}$$

Setting $\epsilon\frac{dR}{dt} = 0$, we obtain a nontrivial steady-state solution for $\epsilon R(t)$, namely

$$\epsilon R = 2.3516\sqrt{24.3344\epsilon\tau_\epsilon - 24.1186\epsilon^2\tau_\epsilon^2}. \tag{6.3}$$

Substituting (6.3) into the second equation of model (6.1) and then integrating yields

$$\phi(t) = \phi_0 + (474.5458\epsilon\tau_\epsilon - 463.1149\epsilon^2\tau_\epsilon^2)t,$$

where ϕ_0 is the initial phase.

In the subsequent analysis, we concentrate on time-varying delay models by employing periodic delay perturbations for oscillation control. Through multiple scale analysis of the time-delayed dynamics, we establish the governing amplitude-frequency equation

$$\begin{cases} \frac{dR}{dt} = P_1(t)R(t) + P_3(t)R^3(t) + O(\epsilon^3), \\ \frac{d\phi}{dt} = P_0(t) + P_2(t)R^2(t) + O(\epsilon^3), \end{cases} \tag{6.4}$$

where $P_1(t) = q_0 + q_{11}\sin(\Omega t) + q_{12}\cos(\Omega t), P_3(t) = -5.5301\epsilon^2, P_0(t) = r_0 + r_{11}\sin(\Omega t) + r_{12}\cos(\Omega t), P_2(t) = 3.8648\epsilon^2$, here $q_0 = -2.5617L^2 + 24.3344\bar{\tau} - 24.1186\bar{\tau}^2, q_{11} = 2.6736\epsilon\tau_\epsilon\Omega L, q_{12} = 3.1239\epsilon\tau_\epsilon\Omega L, r_0 = -2.5927L^2 + 24.5964\bar{\tau} - 24.1186\bar{\tau}^2, r_{11} = 2.6736\epsilon\tau_\epsilon\Omega L$, and $r_{12} = 3.1239\epsilon\tau_\epsilon\Omega L$.

Assuming that $\Omega = 0.02$ and $\epsilon\tau_\epsilon = 0.0001$, by solving $q_0 = 0$, we determine the critical control parameter value L that triggers oscillation attenuation in system, which is $L = 0.9622$. When $L_1 = 0.9906$ exceeds the critical value 0.9622, compared with Figure 9, we observe a reduction in the oscillation amplitude when $t = 50$, as illustrated in Figure 12. When $L_2 = 0.9368 < 0.9622$, the oscillation degree is significantly weakened when $t = 50$ (see Figure 13), and the model becomes stable when $t = 300$ (see Figure14).

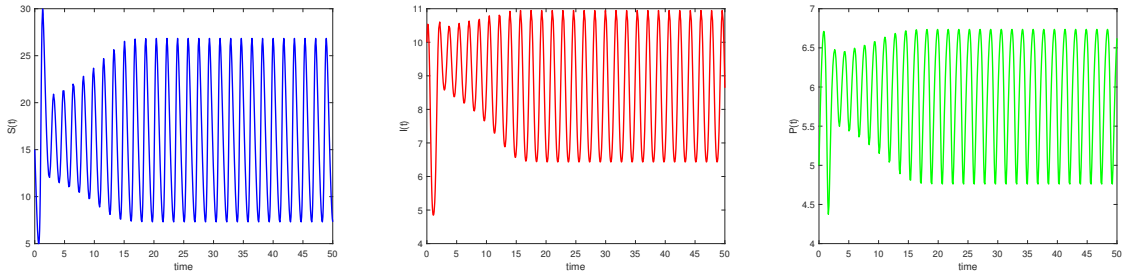

(a) (b) (c)

Figure 12. The oscillation suppression for $L_1 = 0.9906 > 0.9622$. (a) $S(t)$, (b) $I(t)$, and (c) $P(t)$.

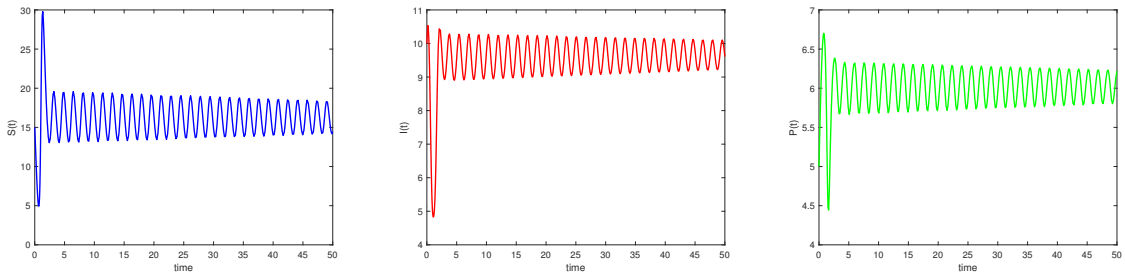

(a) (b) (c)

Figure 13. The oscillation suppression for $L_2 = 0.9368 < 0.9622$. (a) $S(t)$, (b) $I(t)$, and (c) $P(t)$.

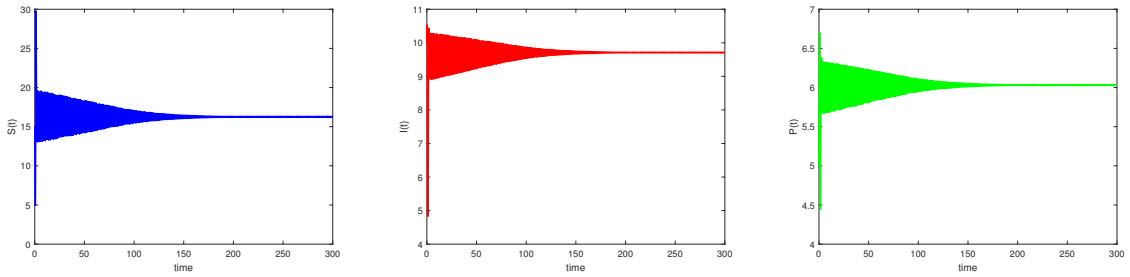

(a) (b) (c)

Figure 14. The oscillation suppression for $L_2 = 0.9388 < 0.9622$. (a) $S(t)$, (b) $I(t)$, and (c) $P(t)$.

The findings presented above indicate that when a time-varying perturbation is implemented on the time delay, the system's oscillatory behavior progressively attenuates and eventually vanishes. This confirms that the oscillation suppression strategy employing periodic delay is effective in this work. Furthermore, when the gestation delay exhibits nearly periodic variations, the instability levels of prey and predator populations gradually diminish, promoting a state of stable coexistence.

7. Discussions and conclusions

Compared with references [11], the most significant improvement of this manuscript lies in the introduction of a generalist predator, transforming a conventional eco-epidemic model into a eco-epidemic model with additional food for predators. This modification yields more complex dynamics and better approximates real-world ecosystems. To improve the model's realism, we interpreted the time delay as the gestation delay, i.e., the period between conception and birth. Furthermore, accounting for factors such as climate, environmental fluctuations, and individual differences, we incorporated a time-varying gestation delay for the generalist predator, replaced the constant delay, and conduct a detailed analysis of its effects on stability using the time-varying delay as a bifurcation parameter. Thus, we considered a time-varying delay eco-epidemic model incorporating additional food, nonlinear prey refuge, and Holling type I functional response. We systematically discussed the dynamical behavior of three system configurations: delay-free, constant-delay, and time-varying delay cases. These theoretical analyses were complemented by numerical simulations implemented through computational software.

First, we established the positivity and boundedness for model (2.1). Subsequently, we conducted a comprehensive local stability analysis of all six equilibriums in the non-delayed case. The local asymptotic stability at the predator-free equilibrium, disease-free equilibrium, and the positive equilibrium are showed in Figure 2(b), Figure 2(c), and Figure 4. Furthermore, we established the global stability of the positive equilibrium by constructing a suitable Lyapunov function, as shown in Figure 5. Subsequently, we examined the stability implications of introducing time-varying delays to the model. For sufficiently small time-varying delays, the positive equilibrium maintains global asymptotic stability, as numerically confirmed in Figure 6. However, beyond critical delay thresholds, such a model undergoes qualitative transitions to complex dynamical regimes, including sustained oscillations, as demonstrated in Figure 7. We noted that a Hopf bifurcation emerges at $\tau = \bar{\tau}$ (see Figure

8). Furthermore, our analysis indicates that for $\tau = 0.2 < \bar{\tau} = 0.2248$, the positive equilibrium of model (4.1) is locally asymptotically stable, as shown in Figure 9. However, when $\tau = 0.24 > \bar{\tau} = 0.2248$, model (4.1) becomes unstable (see Figure 10).

Our investigations reveal that time delay can induce oscillatory dynamics in model (4.1) via Hopf bifurcation mechanisms. In the context of our eco-epidemic model, such sustained oscillations among susceptible prey, infected prey, and predator populations may destabilize the ecological system. Consequently, understanding the oscillation mechanisms and developing suppression strategies becomes imperative. Employing the multiple time scales technique, we obtained a quantitative relationship linking the time delay to the periodic oscillations induced by Hopf bifurcation, along with the threshold perturbation amplitude required to effectively suppress the oscillatory dynamics of the model. As to that shown in Figure 11, when $L_1 = 0.9906 > 0.9622$, the oscillation degree is weakened compared to Figure 10. When $L_2 = 0.9368 < 0.9622$, the oscillation degree is significantly weakened (see Figure 12), and the model becomes stable (see Figure 13). Computational experiments confirm that implementing periodic perturbations to the time delay effectively suppresses oscillatory dynamics in the model, as quantified by amplitude reduction metrics. Our results indicate that time-varying delay perturbations constitute an effective control mechanism for stabilizing these oscillations. This delay-based control methodology provides a theoretically grounded approach for system stabilization, leveraging temporal modulation of feedback delays as the control mechanism. In contrast to references [38, 39], and drawing inspiration from reference [13], we explicitly formulated the predation of generalist predators on additional food resources using a precise mathematical expression, thereby quantifying the impact of additional food resources on ecosystem stability. Finally, informed by references [24–26], we employed the MMS to effectively suppress oscillations.

Our findings of this study carry important implications for real-world ecological conservation. The results show that as the growth rate obtained by predators from additional food (η) increases, the population sizes of susceptible prey, infected prey, and predators all rise. In contrast, when the predators' dependence on additional food (η_0) increases, the sizes of the three populations decline. This implies that conservation measures aimed at enhancing the availability of additional food for predators, while preventing their overdependence on it, can promote species richness and help maintain a high level of ecosystem stability. Appropriately controlling the refuge coefficient can mitigate or eliminate disease transmission. In ecosystem conservation, excessive human intervention, particularly setting an excessively high refuge coefficient, may disrupt system stability and lead to species extinction. Conversely, maintaining a relatively low refuge coefficient contributes to ecological stability.

In summary, this work enhances our comprehension of the dynamics inherent in eco-epidemic models, particularly highlighting how time delay can give rise to intricate dynamical behaviors. However, this study has limitations, and many interesting topics remain to be further investigated. For instance, since disease transmission among prey is not instantaneous and may be influenced by climatic, environmental, and temperature conditions, we can introduce an additional time-varying delay to represent this transmission delay. Moreover, we incorporated susceptible prey's refuge-seeking behavior into the model and investigated its impact on the overall ecosystem dynamics. To model this, we introduced another refuge effect parameterized by "q" (susceptible prey refuge coefficient, which means protecting qS of susceptible prey, and the disease can infect only a proportion $(1-q)S$ of the susceptible prey population). This simulates certain human intervention measures during disease outbreaks in captive animals: When a proportion of susceptible prey is sheltered, the number

of infected prey decreases, leading to a reduction or elimination of the disease, which aids in disease control. It is worthwhile to investigate the following eco-epidemic model with time-varying delay, which incorporates transmission delay and a refuge for susceptible prey:

$$\begin{cases} \dfrac{\mathrm{d}S}{\mathrm{d}t} = rS(1-\dfrac{S+I}{K}) - \dfrac{\beta(1-q)SI}{b+S} - m(1-\delta_1 P)SP + \gamma I - q_1 ES, \\ \dfrac{\mathrm{d}I}{\mathrm{d}t} = \dfrac{\beta(1-q)S(t-\tau_1(t))I(t-\tau_1(t))}{b+S(t-\tau_1(t))} - n(1-\delta_2 P)IP - \gamma I - d_1 I, \\ \dfrac{\mathrm{d}P}{\mathrm{d}t} = \dfrac{\eta P}{1+\eta_0 P} + e_1 m(1-\delta_1 P(t-\tau_2(t)))S(t-\tau_2(t))P(t-\tau_2(t)) \\ \qquad + e_2 n(1-\delta_2 P(t-\tau_2(t)))I(t-\tau_2(t))P(t-\tau_2(t)) - d_2 P - q_2 EP. \end{cases}$$

Further investigation into the dynamics of the above model is required, and this will be pursued in subsequent studies.

Author contributions

Conceptualization, P.-F. Zhou and X.-Y. Meng; methodology, P.-F. Zhou; software, P.-F. Zhou; validation, P.-F. Zhou and X.-Y. Meng; formal analysis, P.-F. Zhou; investigation, P.-F. Zhou and X.-Y. Meng; writing–original draft, P.-F. Zhou; writing–reviewing and editing, P.-F. Zhou and X.-Y. Meng; visualization, P.-F. Zhou and X.-Y. Meng; supervision, X.-Y. Meng. All authors have read and agreed to the published version of the manuscript.

Acknowledgments

This work is supported by the National Natural Science Foundation of China (Grant No. 12161054 and 12361011), Funds for Innovative Fundamental Research Group Project of Gansu Province (Grant No. 24JRRA778), and the Doctoral Foundation of Lanzhou University of Technology.

Conflict of interest

All authors declare no conflicts of interest in this paper.

Use of Generative-AI tools declaration

The authors declare that they have not used Artificial Intelligence (AI) tools in the creation of this article.

Appendix

$$
\begin{aligned}
&F_1(\varphi) = C_{11}\varphi_1^2(0) + C_{12}\varphi_1(0)\varphi_2(0) + C_{13}\varphi_1(0)\varphi_3(0) + C_{14}\varphi_3^2(0),\\
&F_2(\varphi) = C_{21}\varphi_1^2(0) + C_{22}\varphi_1(0)\varphi_2(0) + C_{23}\varphi_2(0)\varphi_3(0) + C_{24}\varphi_3^2(0),\\
&F_3(\varphi) = C_{31}\varphi_3^2(0) + C_{32}\varphi_1(-1)\varphi_3(-1) + C_{33}\varphi_2(-1)\varphi_3(-1) + C_{34}\varphi_3^2(-1),\\
&C_{11} = -\frac{r}{K} + \frac{\beta b I^*}{(b+S^*)^3}, C_{12} = -\frac{r}{K} - \frac{\beta b}{(b+S^*)^2}, C_{13} = 2m\delta_1 P^* - m,\\
&C_{14} = m\delta_1 S^*, C_{21} = -\frac{\beta b I^*}{(b+S^*)^3}, C_{22} = \frac{\beta b}{(b+S^*)^2}, C_{23} = 2n\delta_2 P^* - n,\\
&C_{24} = n\delta_2 I^*, C_{31} = -\frac{\eta\eta_0}{(1+\eta_0 P^*)^3}, C_{32} = e_1 m(1-2\delta_1 P^*),\\
&C_{33} = e_2 n(1-2\delta_2 P^*), C_{34} = -e_1 m\delta_1 S^* - e_2 n\delta_2 I^*.
\end{aligned}
\tag{A1}
$$

$$
\begin{aligned}
k_{11} =& C_{11} + C_{12}q_1 + C_{13}q_2 + C_{14}q_2^2, k_{13} = C_{11} + C_{12}\bar{q}_1 + C_{13}\bar{q}_2 + C_{14}\bar{q}_2^2,\\
k_{12} =& 2C_{11} + C_{12}(q_1+\bar{q}_1) + C_{13}(q_2+\bar{q}_2) + 2C_{14}q_2\bar{q}_2,\\
k_{21} =& C_{21} + C_{22}q_1 + C_{23}q_1q_2 + C_{24}q_2^2, k_{23} = C_{21} + C_{22}\bar{q}_1 + C_{23}\bar{q}_1\bar{q}_2 + C_{24}\bar{q}_2^2,\\
k_{22} =& 2C_{21} + C_{22}(q_1+\bar{q}_1) + 2C_{23}q_1\bar{q}_2 + 2C_{24}q_2\bar{q}_2,\\
k_{31} =& C_{31}q_2^2 + C_{32}q_2e^{-i\omega_k\bar{\tau}} + C_{33}q_1q_2e^{-2i\omega_k\bar{\tau}} + C_{34}q_2^2e^{-2i\omega_k\bar{\tau}},\\
k_{32} =& 2C_{31}q_2\bar{q}_2 + C_{32}(q_2+\bar{q}_2)e^{2i\omega_k\bar{\tau}} + C_{33}(q_1\bar{q}_2+\bar{q}_1q_2)e^{2i\omega_k\bar{\tau}} + 2C_{34}q_2\bar{q}_2e^{2i\omega_k\bar{\tau}},\\
k_{33} =& C_{31}\bar{q}_2^2 + C_{32}\bar{q}_2e^{-i\omega_k\bar{\tau}} + C_{33}\bar{q}_1\bar{q}_2e^{-2i\omega_k\bar{\tau}} + C_{34}\bar{q}_2^2e^{-2i\omega_k\bar{\tau}},\\
k_{14} =& C_{11}(W_{20}^{(1)}(0) + 2W_{11}^{(1)}(0)) + C_{12}(\frac{1}{2}W_{20}^{(1)}(0)\bar{q}_1 + q_1W_{11}^{(1)}(0) + W_{11}^{(2)}(0) + \frac{1}{2}W_{20}^{(2)}(0))\\
&+ C_{13}(\frac{1}{2}W_{20}^{(1)}(0)\bar{q}_2 + q_2W_{11}^{(1)}(0) + W_{11}^{(3)}(0) + \frac{1}{2}W_{20}^{(3)}(0)) + C_{14}(W_{20}^{(3)}(0) + 2W_{11}^{(3)}(0)),\\
k_{24} =& C_{21}(W_{20}^{(1)}(0) + 2W_{11}^{(1)}(0)) + C_{22}(\frac{1}{2}W_{20}^{(1)}(0)\bar{q}_1 + q_1W_{11}^{(1)}(0) + W_{11}^{(2)}(0) + \frac{1}{2}W_{20}^{(2)}(0))\\
&+ C_{23}(\frac{1}{2}W_{20}^{(2)}(0)\bar{q}_2 + q_2W_{11}^{(1)}(0) + q_1W_{11}^{(3)}(0) + \frac{1}{2}\bar{q}_1W_{20}^{(3)}(0))\\
&+ C_{24}(W_{20}^{(3)}(0) + 2W_{11}^{(3)}(0)),\\
k_{34} =& C_{31}(W_{20}^{(3)}(0) + 2W_{11}^{(3)}(0)) + C_{32}(\frac{1}{2}W_{20}^{(3)}(-1) + W_{11}^{(3)}(-1) + q_2e^{i\omega_k\bar{\tau}}W_{11}^{(1)}(-1)\\
&+ \frac{1}{2}\bar{q}_2e^{-i\omega_k\bar{\tau}}W_{20}^{(1)}(-1)) + C_{33}(\frac{1}{2}\bar{q}_1W_{20}^{(3)}(-1) + q_1W_{11}^{(3)}(-1) + q_2e^{i\omega_k\bar{\tau}}W_{11}^{(2)}(-1)\\
&+ \frac{1}{2}\bar{q}_2e^{-i\omega_k\bar{\tau}}W_{20}^{(2)}(-1)) + C_{34}(W_{20}^{(3)}(-1) + 2W_{11}^{(3)}(-1)).
\end{aligned}
\tag{A2}
$$

$$
\begin{aligned}
g_2 =& F_{U_\tau}(\frac{1}{2}\bar{\tau}^2 D_{11}U_{1\tau} + \frac{1}{2}\tau_\epsilon^2 D_{00}U_{1\tau} + \tau_\epsilon\bar{\tau}D_{01}U_{1\tau} - \bar{\tau}D_2U_{1\tau} - \bar{\tau}D_1U_{2\tau} \\
& - \tau_\epsilon D_1U_{1\tau} - \tau_\epsilon D_0U_{2\tau}) + F_{UU}U_1U_2 + F_{UU_\tau}(U_{1\tau}U_2 + U_1(U_{2\tau} - \bar{\tau}D_1U_{1\tau} \\
& - \tau_\epsilon D_0U_{1\tau})) + U_{1\tau}F_{U_\tau U_\tau}(U_{2\tau} - \bar{\tau}D_1U_{1\tau} - \tau_\epsilon D_0U_{1\tau}) + \frac{1}{2}F_{UUU_\tau}U_1^2U_{1\tau} \\
& + \frac{1}{2}F_{UU_\tau U_\tau}U_1U_{1\tau}^2 + \frac{1}{6}F_{U_\tau U_\tau U_\tau}U_{1\tau}^3 + \frac{1}{6}F_{UUU}U_1^3 - D_2U_1 - D_1U_2 \\
=& F_{U_\tau}(\frac{1}{2}\bar{\tau}^2 D_{11}(M_1\sin(\omega(T_0-\bar{\tau})) + N_1\cos(\omega(T_0-\bar{\tau}))) \\
& + \frac{1}{2}\tau_\epsilon^2(-\omega^2M_1\sin(\omega(T_0-\bar{\tau})) - \omega^2N_1\cos(\omega(T_0-\bar{\tau}))) \\
& + \tau_\epsilon\bar{\tau}(\omega D_1M_1\cos(\omega(T_0-\bar{\tau})) - \omega D_1N_1\sin(\omega(T_0-\bar{\tau}))) \\
& - \bar{\tau}D_2(M_1\sin(\omega(T_0-\bar{\tau})) + N_1\cos(\omega(T_0-\bar{\tau}))) \\
& - \bar{\tau}D_1(M_2\sin(2\omega(T_0-\bar{\tau})) + N_2\cos(2\omega(T_0-\bar{\tau})) + O_2) \\
& - \tau_\epsilon D_1(M_1\sin(\omega(T_0-\bar{\tau})) + N_1\cos(\omega(T_0-\bar{\tau}))) \\
& - \tau_\epsilon 2\omega(M_2\cos(2\omega(T_0-\bar{\tau})) - N_2\sin(2\omega(T_0-\bar{\tau}))) \\
& + F_{UU}(M_1\sin(\omega T_0) + N_1\cos(\omega T_0))(M_2\sin(2\omega T_0) + N_2\cos(2\omega T_0) + O_2) \\
& + F_{UU_\tau}(M_1\sin(\omega(T_0-\bar{\tau})) + N_1\cos(\omega(T_0-\bar{\tau})))(M_2\sin(2\omega T_0) \\
& + N_2\cos(2\omega T_0) + O_2) + F_{UU_\tau}(M_1\sin(\omega T_0) + N_1\cos(\omega T_0)) \\
& (M_2\sin(2\omega(T_0-\bar{\tau})) + N_2\cos(2\omega(T_0-\bar{\tau})) + O_2) - F_{UU_\tau}(M_1\sin(\omega T_0)) \\
& (\bar{\tau}D_1(M_1\sin(\omega(T_0-\bar{\tau})) + N_1\cos(\omega(T_0-\bar{\tau})))) - F_{UU_\tau}(N_1\cos(\omega T_0)) \\
& (\bar{\tau}D_1(M_1\sin(\omega(T_0-\bar{\tau})) + N_1\cos(\omega(T_0-\bar{\tau})))) - F_{UU_\tau}(M_1\sin(\omega T_0)) \\
& (\tau_\epsilon\omega M_1\cos(\omega(T_0-\bar{\tau})) - \tau_\epsilon\omega N_1\sin(\omega(T_0-\bar{\tau}))) - F_{UU_\tau}(N_1\cos(\omega T_0)) \\
& (\tau_\epsilon\omega M_1\cos(\omega(T_0-\bar{\tau})) - \tau_\epsilon\omega N_1\sin(\omega(T_0-\bar{\tau}))) + F_{U_\tau U_\tau}(M_1\sin(\omega(T_0-\bar{\tau})) \\
& + N_1\cos(\omega(T_0-\bar{\tau})))(M_2\sin(2\omega(T_0-\bar{\tau})) + N_2\cos(2\omega(T_0-\bar{\tau})) + O_2 \\
& - \bar{\tau}D_1M_1\sin(\omega(T_0-\bar{\tau})) - \bar{\tau}D_1N_1\cos(\omega(T_0-\bar{\tau})) - \tau_\epsilon\omega M_1\cos(\omega(T_0-\bar{\tau})) \\
& + \tau_\epsilon\omega N_1\sin(\omega(T_0-\bar{\tau}))) + \frac{1}{2}F_{UUU_\tau}(M_1\sin(\omega T_0) + N_1\cos(\omega T_0))^2 \\
& (M_1\sin(\omega(T_0-\bar{\tau})) + N_1\cos(\omega(T_0-\bar{\tau}))) + \frac{1}{2}F_{UU_\tau U_\tau}(M_1\sin(\omega T_0) \\
& + N_1\cos(\omega T_0))(M_1\sin(\omega(T_0-\bar{\tau})) + N_1\cos(\omega(T_0-\bar{\tau})))^2 \\
& + \frac{1}{6}F_{U_\tau U_\tau U_\tau}(M_1\sin(\omega(T_0-\bar{\tau})) + N_1\cos(\omega(T_0-\bar{\tau})))^3 \\
& + \frac{1}{6}F_{UUU}(M_1\sin(\omega T_0) + N_1\cos(\omega T_0))^3 - D_2(M_1\sin(\omega T_0) \\
& + N_1\cos(\omega T_0)) - D_1(M_2\sin(2\omega T_0) + N_2\cos(2\omega T_0) + O_2),
\end{aligned}
\tag{A3}
$$

References

1. A. Lotka, Analytical note on certain rythmic relations in organic systems, *Proc. Nat. Acad. Sci.* **6** (1920), 410–415. https://doi.org/10.1073/pnas.6.7.410

2. V. Volterra, Variations and fluctuations of the number of individuals in animal species living together, Animal Ecology, *ICES. J. Mar. Sci.*, **3** (1928), 3–51. https://doi.org/10.1093/icesjms/3.1.3

3. R. Ma, X. Meng, Dynamics of an eco-epidemiological model with toxicity, treatment,time-varying incubation, *Electron. Res. Arch.*, **33** (2025), 3074–3110. https://doi.org/10.3934/era.2025135

4. X. Zhang, R. Ning, Threshold dynamics of a stochastic tumor-immune model with adoptive cell transfer therapy, *Qualit. Theo. Dyn. Syst.*, **25** (2026), 82. https://doi.org/10.1007/s12346-026-01505-0

5. X. Liu, X. Meng, Dynamics of Bacterial white spot disease spreads in Litopenaeus Vannamei with time-varying delay, *Math. Biosci. Eng.*, **20** (2023), 20748–20769. https://doi.org/10.3934/mbe.2023918

6. J. Wang, X. Meng, X. Lei, Bifurcations and control for plant-herbivore systems with spatiotemporal nonlocal effects in arid regions, *Int. J. Bifurcat. Chaos*, **396** (2026), 109659. https://doi.org/10.1142/S0218127426500719

7. E. Beltrami, T. Carroll, Modelling the role of viral disease in recurrent phytoplankton blooms, *J. Math. Biol.*, **32** (1994), 857–863. https://doi.org/10.1007/bf00168802

8. X. Meng, N. Qin, H. Huo, Dynamics analysis of a predator-prey system with harvesting prey and disease in prey species, *J. Biol. Dyn.*, **12** (2018), 342–374. https://doi.org/10.1080/17513758.2018.1454515

9. N. Sk, S. Pal, Dynamics of an infected prey-generalist predator system with the effects of fear, refuge and harvesting: deterministic and stochastic approach, *Eur. Phys. J. Plus.*, **137** (2022), 1–24. https://doi.org/10.1140/epjp/s13360-022-02348-9

10. C. Holling, The components of predation as revealed by a study of small-mammal predation of the european pine sawfly, *Can. Entomol.*, **91** (1959), 293–320. https://doi.org/10.4039/Ent91293-5

11. M. Islam, N. Sk, S. Sarwardi, Deterministic and stochastic study of an eco-epidemic predator-prey model with nonlinear prey refuge and predator harvesting, *Eur. Phys. J. Plus.*, **138** (2023), 851. https://doi.org/10.1140/epjp/s13360-023-04476-2

12. C. Jana, A. Maiti, D. Maiti, Complex dynamical behavior of a ratio-dependent eco-epidemic model with holling type-II incidence rate in the presence of two delays, *Commun. Nonlinear Sci. Numer. Simul.*, **110** (2022), 106380. https://doi.org/10.1016/j.cnsns.2022.106380

13. A. Erbach, F. Lutscher, G. Seo, Bistability and limit cycles in generalist predator-prey dynamics, *Ecol. Complex.*, **14** (2013), 48–55. https://doi.org/10.1016/j.ecocom.2013.02.005

14. R. Beverton, S. Holt, On the Dynamics of Exploited Fish Populations, Springer Netherlands, 1993. https://doi.org/10.1007/978-94-011-2106-4

15. M. Islam, B. Mondal, S. Sarwardi, Integrated dynamics of eco-epidemic systems: Nonlinear prey refuge, predator exploitation, fear impact, and infection control, *Braz. J. Phys.*, **55** (2025), 115. https://doi.org/10.1007/s13538-025-01744-7

16. Y. Zhang, N. Wei, F. Lai, S. Gao, Y. Luo, Mathematical analysis of a two-patch eco-epidemiological predator-prey model with fear effects and a generalized ratio-dependent functional response, *J. Appl. Math. Comput.*, **72** (2026), 106. https://doi.org/10.1007/s12190-025-02761-0

17. I. Barbalat, System equations differentielle oscillations non linearies, *Rev. Roumaine Math. Pures Appl.*, **4** (1959), 267–270.

18. P. Yuan, L. Chen, M. You, H. Zhu, Dynamics complexity of generalist predatory mite and the leafhopper pest in tea plantations, *J. Dyn. Differ. Equ.*, **35** (2023), 2833–2871. https://doi.org/10.1007/s10884-021-10079-1

19. S. Fan, A new extracting formula and a new distinguishing means on the one variable cubic equation, *Nat. Sci. J. Hainan Univ.*, **2** (1989), 91–98.

20. B. Hassard, N. Kazarinoff, Y. Wan, Therory and Applications of Hopf Bifurcation, Cambridge University Press, Cambridge, 1981.

21. R. Goodrich, A Riesz representation theorem, *Proc. Amer. Math. Soc.*, **24** (1970), 629–636. https://doi.org/https://doi.org/10.1090/s0002-9939-1970-0415386-2

22. X. Meng, Z. Liang, Dynamics analysis of a delayed diffusive predator-prey model with memory-based diffusion and fear effect of prey, *Int. J. Biomath.*, (2025). https://doi.org/10.1142/S1793524525501013

23. X. Meng, X. Sun, Dynamics of a stage-structure diffusive predator-prey model with nonlinear prey refuge, delay and anti-predator behavior, *Int. J. Appl. Comput. Math.*, **12** (2026), 2. https://doi.org/10.1007/s40819-025-02077-4

24. S. Das, A. Chatterjee, Multiple scales without center manifold reductions for delay differential equations near Hopf bifurcations, *Nonlinear Dyn.*, **30** (2002), 323–335. https://doi.org/10.1023/a:1021220117746

25. S. Zhang, J. Xu, Oscillation control for n-dimensional congestion control model via time-varying delay, *Sci. China Technol. Sci.*, **54** (2011), 2044–2053. https://doi.org/10.1007/s11431-011-4488-8

26. L. Pei, Y. Chen, S. Wang, Complicated oscillations and non-resonant double Hopf bifurcation of multiple feedback delayed control system of the gut microbiota, *Nonlinear Anal. Real World Appl.*, **54** (2020), 103091. https://doi.org/10.1016/j.nonrwa.2020.103091

27. X. Meng, R. Ma, Dynamics of a time-varying delay Beddington-DeAngelis prey-predator model with fear effect and anti-predator behaviour, *Diff. Equat. Dyn. Syst.*, **2025** (2025), 1–43. https://doi.org/10.1007/s12591-025-00729-x

28. N. Thakur, S. Srivastava, A. Ojha, Dynamical study of an ecoepidemiological delay model for plankton system with toxicity, *Iran. J. Sci. Technol. Trans. A Sci.*, **45** (2021), 283–304. https://doi.org/10.1007/s40995-020-01042-8

29. S. Biswas, P. Tiwari, Delay-induced chaos and its possible control in a seasonally forced eco-epidemiological model with fear effect and predator switching, *Nonlinear Dyn.*, **104** (2021), 2901–2030. https://doi.org/10.1007/s11071-021-06396-1

30. D. Li, H. Liu, H. Zhang, Bifurcation analysis in a predator-prey model with an Allee effect and a delayed mechanism, *Acta Math. Sci.*, **43** (2023), 1415–1438. https://doi.org/10.1007/s10473-023-0324-z

31. M. Huang, X. Song, Modeling and qualitative analysis of diabetes therapies with state feedback control, *Int. J. Biomath.*, **7** (2014), 1450035. https://doi.org/10.1142/S1793524514500351

32. V. Sharma, A. Singh, Strong resonance bifurcations and state feedback control in a discrete prey-predator model with harvesting effect, *Qual. Theory Dyn. Syst.*, **22** (2023), 109. https://doi.org/10.1007/s12346-023-00805-z

33. K. Pyragas, Delayed feedback control of chaos, *Philos. Trans. R. Soc. A Math. Phys. Eng. Sci.*, **364** (2006), 2309–2334. https://doi.org/10.1098/rsta.2006.1827

34. X. Meng, P. Zhou, Stability and bifurcation of a time-varying delay generalist food chain model with double fear effect, *Math. Meth. Appl. Sci.*, (2026), 1–33. https://doi.org/10.1002/mma.70809

35. M. Shabbir, Q. Din, Understanding cannibalism dynamics in predator-prey interactions: Bifurcations and chaos control strategies, *Qual. Theory Dyn. Syst.*, **23** (2024), 1–33. https://doi.org/10.1007/s12346-023-00908-7

36. X. Zhang, Q. Zhang, Bifurcation analysis and control of a class of hybrid biological economic models, *Nonlinear Anal. Hybrid Syst.*, **3** (2009), 578–587. https://doi.org/10.1016/j.nahs.2009.04.009

37. Y. Zheng, Z. Wang, Stability analysis of nolinear dynamics systems with slowly and periodically varying delay, *Commun. Nonlinear Sci. Numer. Simul.*, **17** (2012), 3999–4009. https://doi.org/10.1016/j.cnsns.2012.02.026

38. N. Kumari, V. Kumar, Controlling chaos and pattern formation study in a tritrophic food chain model with cannibalistic intermediate predator, *Eur. Phys. J. Plus.*, **137** (2022), 1–23. https://doi.org/10.1140/epjp/s13360-022-02539-4

39. H. Verma, K. Antwi-Fordjour, M. Hossain, N. Pal, RD. Parshad, P. Mathur, A "Double" fear effect in a tri-trophic food chain model, *Eur. Phys. J. Plus.*, **136** (2021), 1–17. https://doi.org/10.1140/epjp/s13360-021-01900-3

AIMS Press